Developmental rules of primate dental evolution align microevolution with macroevolution

Fabio A. Machado[a,1], **Carrie S. Mongle**[b], **Graham Slater**[c], **Anna Penna**[d], **Anna Wisniewski**[c], **Anna Soffin**[a], **Vitor Dutra**[e], **and Josef C. Uyeda**[a]

[a]Department of Biology, Virginia Tech, VA.; [b]Department of Anthropology, Stony Brook University, NY.; [c]Department of Geophysical Sciences, University of Chicago, IL.; [d]Department of Anthropology, University of Texas at San Antonio, TX.; [e]Department of Anthropology, Florida Atlantic University , FL

This manuscript was compiled on August 19, 2022

Studies of macroevolution have classically rejected the notion that large-scale divergence patterns can be explained through populational, microevolutionary models. For morphology, this consensus partly derives from the inability of quantitative genetics models to correctly predict the behavior of evolutionary processes at the scale of millions of years. Developmental studies (evo-devo) have been proposed to reconcile micro and macroevolution. However, there has been little progress in establishing a formal framework to apply evo-devo models of phenotypic diversification. Here, we reframe this issue by asking if using evo-devo models to quantify biological variation can improve the explanatory power of comparative models, thus helping us bridge the gap between micro- and macroevolution. We test this prediction by evaluating the evolution of primate lower molars in a comprehensive dataset densely sampled across living and extinct taxa. Our results suggest that biologically-informed morphospaces alongside quantitative genetics models allow a seamless transition between the micro and macro scales, while biologically uninformed spaces do not. We show that the adaptive landscape for primate teeth is corridor-like, with changes in morphology within the corridor being nearly neutral. Overall, our framework provides a basis for integrating evo-devo into the modern synthesis, allowing an operational way to evaluate the ultimate causes of macroevolution.

Macroevolution | Microevolution | Evo-Devo | Inhibitory Cascade Model | Morphospace

DRAFT

"Macroevolution" is the field of study which aims to understand how the diversification of life occurred on our planet over large time scales (1). Like any other historical science, it seeks to make sense of patterns over time ingrained in the fossil record and phylogenetic trees by referencing well-understood processes known from direct observations and experimentation (2). In the case of evolutionary biology, this knowledge comes from fields such as ecology and genetics, which tend to map evolutionary phenomena in shorter time scales. For this reason, these studies have been conventionally called "microevolution" and are better suited to understanding the intricacies of how population-level phenomena can produce evolutionary change. However, despite the presumed direct relationship between micro- and macro levels, quantitative studies have struggled to explain most macroevolutionary patterns in terms of microevolutionary processes (3–6). This struggle has led to a number of paradoxes that remain the source of intense debate, with some arguing for the essential irreconcilability of both levels (3, 7, 8) and others advocating for reconciliation within the context of the modern synthesis (5, 9–15).

Despite recent advances in phylogenetic comparative methods, models of trait evolution remain largely phenomenological in their description of macroevolutionary patterns (16), hindering a direct interpretation in microevolutionary terms. Commonly used models such as Brownian Motion (BM) and Ornstein-Uhlenbeck (OU) models can emerge from simple extrapolation of microevolutionary processes such as genetic drift and drift-selection balance around a stationary optimum, respectively– but many other processes can lead to similar dynamics (*e.g.*, random movement of the adaptive

F.A.M., C.S.M. and J.C.U. conceptualize the project. J.C.U. gathered the necessary funds. F.A.M., C.S.M., A.P., A.S. and V.D. gathered the dataset. F.A.M. performed analysis and produced the first draft. F.A.M., C.S.M., A.P., G.S. and J.C.U. wrote the following versions. All authors approved the last draft.

The author's declare no competing interests.

[2] To whom correspondence should be addressed. E-mail: FAM: fmachado@vt.edu

optimum) (17–19). Thus, progress on connecting micro and macroevolutionary scales has required evaluation based not only on model support, but also quantitative evaluation of the plausibility of parameter estimates (20, 21). Since such parameters have biological meaning and can be estimated outside of macroevolutionary data, they provide a mechanism to ground-truth interpretations of macroevolutionary patterns (21). Previous work has shown that such attempts rarely align quantitatively (6, 22) – yet enigmatically are often aligned qualitatively in the relative magnitudes of quantitative genetic variation and macroevolutionary divergence across traits (6, 20, 23–25). It is perhaps unsurprising that simplistic homogenous models naïvely extrapolated to million-year timescales will fail given the inherent heterogeneity of biotic and abiotic change over time. Despite this, such heterogeneities might not affect all traits equally, and finding such traits is a central pursuit of evolutionary biology.

One long-standing suggestion for bridging the gap between micro- and macroevolution has been through the study of developmental biology and ontogeny (*i.e.* evo-devo) (12, 26–28). The existence of deeply canalized developmental modules suggest a long history of stable selective pressures, and may be the most likely place to identify simple connections between micro and macroevolutionary scales–at least once non-linearities inherent to the developmental program are accounted for (29, 30). For these reasons, one might expect that incorporation of developmental knowledge in defining morphospaces can maximize our ability to connect micro and macroevolution–provided sufficient data are available. This suggestion, however, does not come without its hurdles. In a microevolutionary context, development can be taken as a moderately smooth genotype-to-phenotype (GP) map, allowing the modeling of evolution and adaptation of the adult phenotype using the quantitative genetic framework of the adaptive landscape (11–13, 31, 32). On larger time scales, genetic architectures can change, selection can fluctuate, and development can be reorganized, generating non-linearities between genotypic and phenotypic divergence that impedes the straightforward extrapolation of microevolutionary processes over million-year timescales (12, 28, 30, 32, 33). However, absent an understanding of the development and the GP map, it is likely that macroevolutionary studies will find heterogeneity and discontinuities of what may be relatively smooth or continuous underlying genetic changes at the microevolutionary scale (12).

Here, we test the hypothesis that morphological spaces (morphospaces) specifically designed to quantify developmental phenomena maximize our ability to seamlessly connect micro and macroevolutionary scales (12, 33–37). This perspective contrasts with the regular practice of constructing morphospaces as comprehensive, phenomenological, and statistical descriptors of biological form without a clear connection to underlying biological processes (12, 37–39). Notably, such biologically naïve spaces might lead to complex non-linear GP maps, thus hampering the extension of microevolutionary processes to macroevolutionary scales (30, 37, 40, 41). The objective of the present contribution is to show that the quantification of developmentally-informed variables coupled with quantitative genetics modeling and comparative methods can facilitate a conceptual bridge between scales. We present here an extensive synthesis of new and published data on primate molars across scales that establishes, to our knowledge, the first study system that jointly satisfies all the requirements necessary to adequately evaluate these hypotheses.

Specifically, primate molars are among the exceptionally few traits for which extensive direct measurements across scales of time (living and extinct) can be placed phylogenetically and combined with well-characterized genetic architecture and developmental pathways. First, the molar row constitutes a complex trait containing three individual elements (first, second, and third molars – m1, m2, and m3, respectively) that are serially homologous and are formed only once during the development. Once emerged, each molar has a fixed morphology (besides wear)– insulating these

DRAFT

structures from additional environmental variation–and therefore providing a tighter relation between morphology and underlying developmental factors (36). Second, several studies have characterized the additive genetic variation in molars, a key parameter used to predict the molar row response to main microevolutionary processes such as drift and selection (42–45). Third, tooth enamel is the most mineralized substance in vertebrate tissues, making teeth specially resistant to taphonomic processes and abundant in the fossil record. The use of a dense fossil record allows us bridge any phylogenetic gaps between extant species, ensuring that heterogeneities along the tree are indeed due to differences in process, rather than incomplete sampling. This extensive availability of a comprehensive combination of paleontological and neontological data enables unprecedented power to evaluate evolutionary dynamics through deep-time using data-hungry phylogenetic comparative methods (46–48). Lastly and more importantly, there is a simple yet powerful evo-devo model that describes the development and evolution of the mammalian molars, the inhibitory cascade model (ICM). The ICM models teeth proportions (*i.e.* molar row shape) as the result of a balance between inhibition and activation factors, and predicts a positive relationship between the ratios of the areas of the last two molars in relation to the first one (m2/m1 and m3/m1, 36).

Previous investigations have shown that primate dental evolution follows some of the ICM's (mostly macroevolutionary) predictions (25, 49, 50). Here we expand upon these findings by explicitly modeling the macroevolution of primate molars according to microevolutionary models. We compare these models to state-of-the-art phenomenological comparative models that can account for the wide variety of rate and state-heterogenous evolutionary processes. We aim to evaluate whether evo-devo-inspired spaces (i.e. the one implied by the ICM) lead to a smoother transition between micro- and macroevolutionary scales than biologically naïve spaces, which are here represented by linear measurements or areas designed to describe the form of the molar row (Fig S1). We apply this framework to an expansive dataset of both extant (232 taxa) and extinct (248 taxa) species summarized from more than 250 different sources (see Supplementary Material), integrated with a newly published comprehensive phylogenetic context (51).

DRAFT

Results

The use of biologically naïve morphospaces (i.e., linear distances and areas, fig. S2A-B) favored model complexity. Specifically, the best model for these spaces was a multi-regime multivariate BM model, which allows for rate heterogeneity along the tree (Table 1, S1,S2). For molar occlusal areas, the best model had three main regimes (Fig 1). The first regime covers most fossil groups (thus named "ancestral regime"), including Plesiadapiformes, stem-Haplorhini, part of stem-Simiiformes and Tarsiidae. The second regime refers to Strepsirrhini, both crown and stem, and the third refers to crown Simiiformes (monkeys and apes, including humans). For linear distances, this regime combination had better fit than any global model (microevolutionary inspired or not), even though it was not the best solution found for this morphospace (see Supplementary Information, Table S2). In both morphospaces, the ancestral regime accumulated more variance over time than any derived regime, suggesting a weaker constraint on the former (Fig S8). It may be tempting to assign interpretations that are either biological (e.g. higher divergence rates after the K-Pg extinction event resulting from ecological opportunity) or statistical in nature (e.g. increased phylogenetic uncertainty of fossil placement resulting in upwardly biased rates 52). However, we find that such patterns do not appear universally across morphospaces.

By contrast, investigation of evo-devo-inspired variables based on the ICM paints a strikingly different picture (Fig. S2C). Instead of privileging more complex and heterogeneous models, the ICM morphospace identifies a global OU process that incorporates microevolutionary assumptions

Table 1. Comparison of models of primate lower row evolution fit through Maximum Likelihood.

Traits[a]	Model[b]	k [c]	logLik [d]	BIC [e]
Linear distances	BM	27	2585.03	-5003.38
	OU	54	2684.57	-5035.75
	$BM_{\Sigma \propto P}$	7	2108.57	-4173.93
	$OU_{\Sigma \propto P}$	34	2174.45	-4138.99
	$BM_{\Sigma \propto G}$	7	1480.63	-2918.04
	$OU_{\Sigma \propto G}$	34	1510.57	-2811.23
	Three-regime BM [f]	74	2823.03	**-5189.20** [g]
Areas	BM	9	415.80	-776.03
	OU	18	413.98	-716.83
	$BM_{\Sigma \propto P}$	4	92.39	-160.09
	$OU_{\Sigma \propto P}$	13	275.16	-470.06
	$BM_{\Sigma \propto G}$	4	74.41	-124.13
	$OU_{\Sigma \propto G}$	13	258.02	-435.78
	Three-regime BM [f]	26	471.42	**-782.32** [g]
ICM	BM	5	589.16	-1147.46
	OU^D	9	604.56	<u>-1153.55</u> [h]
	$BM_{\Sigma \propto P}$	3	538.31	-1058.10
	$OU_{\Sigma \propto P}$	8	584.68	-1119.98
	$BM_{\Sigma \propto G}$	3	575.69	-1132.86
	$OU^D_{\Sigma \propto G}$	7	598.54	**-1153.86** [g]
	Three-regime OU [f]	26	597.35	-1034.18

[a] Morphospace used to quantify molar form variation; either a biologically naïve space (linear distances or areas) or an evo-devo inspired space (ICM)

[b] Model type. Either global BM or OU models or a mixed model, which allows model and parameter heterogeneity. BM and OU can also incorporate the microevolutionary assumption that the evolutionary rate matrix (Σ) is proportional to G or P ($\Sigma \propto G$ or P models). Uppercase "D" indicates OU models with a diagonal H

[c] Number of model parameters.

[d] Log-likelihood of the model

[e] Bayesian Information Criterion used for model comparison

[f] Results for the mixed model for Linear distances and ICM are based on the best regime combination found for the areas morphospace

[g] Bold represents the best models

[h] Underline represents the ones with BIC 2 units away from the best model.

DRAFT

($OU_{\Sigma \propto G}$; Table 1, S3). Specifically, this best model assumes an evolutionary rate matrix (Σ) proportional to the additive genetic covariance matrix of the traits (**G**-matrix; equations 1,2). Furthermore, parameter estimates of this component are within the range of values consistent with genetic drift around a single stationary optimum (53, 54).

According to the best model, the variation introduced by drift is aligned with the distribution of phenotypes on the ICM morphospace (Fig. 2A), suggesting that the similarity between intra and interspecific patterns of trait variation (see 25) is consistent with drift. This is further reinforced by the investigation of node-specific rates of evolution, which shows a huge overlap with rates expected under genetic drift (Fig 3). However, drift alone would generate more variation than the total observed disparity during the period in which primates have evolved (Fig. S7), suggesting that stabilizing selection played a crucial role in shaping the pattern of evolution in the group.

The investigation of the adaptive landscape implied by the best model shows that stabilizing selection is also aligned with the interspecific distribution of phenotypes (Fig. 2B). An investigation of the half-lives ($t_[1/2]$) in different directions of this adaptive landscape shows that $t_[1/2]$ are higher along the activation-inhibition gradient direction of the ICM and lower in directions that would lead to deviations from the ICM S5. These results suggest that the macroevolution of primate teeth is being being shaped by a strong stabilizing selection against deviation from the ICM pattern, while allowing evolution to occur along the activation-inhibition gradient, in a corridor-like manner.

Discussion

Previous works have usually highlighted that larger-scale morphological evolution tends to conform to the expectation of microevolutionary models qualitatively, but rarely (if ever) in terms of magnitudes of change (6). In other words, while macroevolution seems to follow the directions with more genetic variation, as expected due to neutral change (6, 24, 25, 55–57), rates of evolution tend to fall below those expected under genetic drift (6, 15, 20, 58). This paradox has been used to argue for a fundamental mismatch between micro and macroevolution, as simplistic quantitative genetics models seem unlikely to represent million-year evolutionary processes (18, 20, 59). Here, we constrained the proportionality parameter for the model to be within realistic values (equation 2), resulting in an estimated rate matrix that is compatible with drift around a stationary adaptive peak not only in patterns of trait association, but also in magnitude. The key modeling choice that lead to this conclusion was the quantification of developmentally-informed traits, which smoothed out transitions between microevolutionary and macroevolutionary data–defining and identifying a neutral subspace aligned with a conserved developmental process.

Within the set of microevolutionary-inspired models, OU models outperformed the BM models (Table 1), even though they produced similar estimates of evolutionary rates (Tables S6–S9). This suggests two things. First, that irrespective of which model better fits the data, our dense fossil sample allows us to retrieve precise evolutionary parameter estimates. Second, it suggests that stabilizing selection plays a crucial role in shaping macroevolutionary patterns. Considering the amount of variation introduced by drift every Myr (Fig 2A), a purely neutral process would result in overdispersion of tip values and higher phylogenetic signals (Fig S7). Instead, the patterns of stabilizing selection seem to be essential in shaping the ICM pattern. Stabilizing selection both constrains variation that deviates from the ICM pattern and facilitates evolution along the activation-inhibition gradient (Fig S5,S6). This is further illustrated by the inferred adaptive landscape, which produces an almost corridor-like topology aligned with the ICM pattern (Fig 2B). This corridor seems to have a smooth topography as, despite finding global evidence for stabilizing selection, dense sampling over node-specific rates of evolution calculated throughout the tree are compatible with those expected under drift (Fig 3), a pattern rarely seen for macroevolutionary data (6, 15, 20, 58).

Together, these results point to the interplay of genetic variation, selection, and development leading to a homogeneous macroevolutionary processes within a defined subspace. It has been argued that selection can mold genetic patterns of trait association and variation (31, 60, 61), specifically by molding developmental pathways and genetic interactions (62, 63). Conversely, development has also been argued to impose direct selective pressures (*i.e.* internal selection) by reducing the viability of non-conforming phenotypes (31, 64) which could, in turn, trickle down to the organization of genetic variation. While in the present case we can observe this triple alignment between genetics, ontogeny and selection, its origins are harder to decipher. The ICM was originally described in rodents and later verified in many other mammalian groups (65, 66), suggesting it is the ancestral condition. In this case, ontogeny is viewed as the organizing factor behind both selective patterns and the organization of genetic variation (25). Furthermore, this explains the near-neutral quality of primate dental evolution, as conformity to the developmental process would be the main selective pressure on relative tooth sizes. However, some mammalian groups have been shown to deviate from the predictions of the ICM to different degrees, suggesting that the ontogenetic process itself could be malleable (65–69). Indeed, it has been argued that molar tooth eruption timing in Primates is shaped by biomechanical demands at different ontogenetic stages (70), revealing a possible mechanism through which external selection could shape development, and indirectly, the morphology of the molar row.

DRAFT

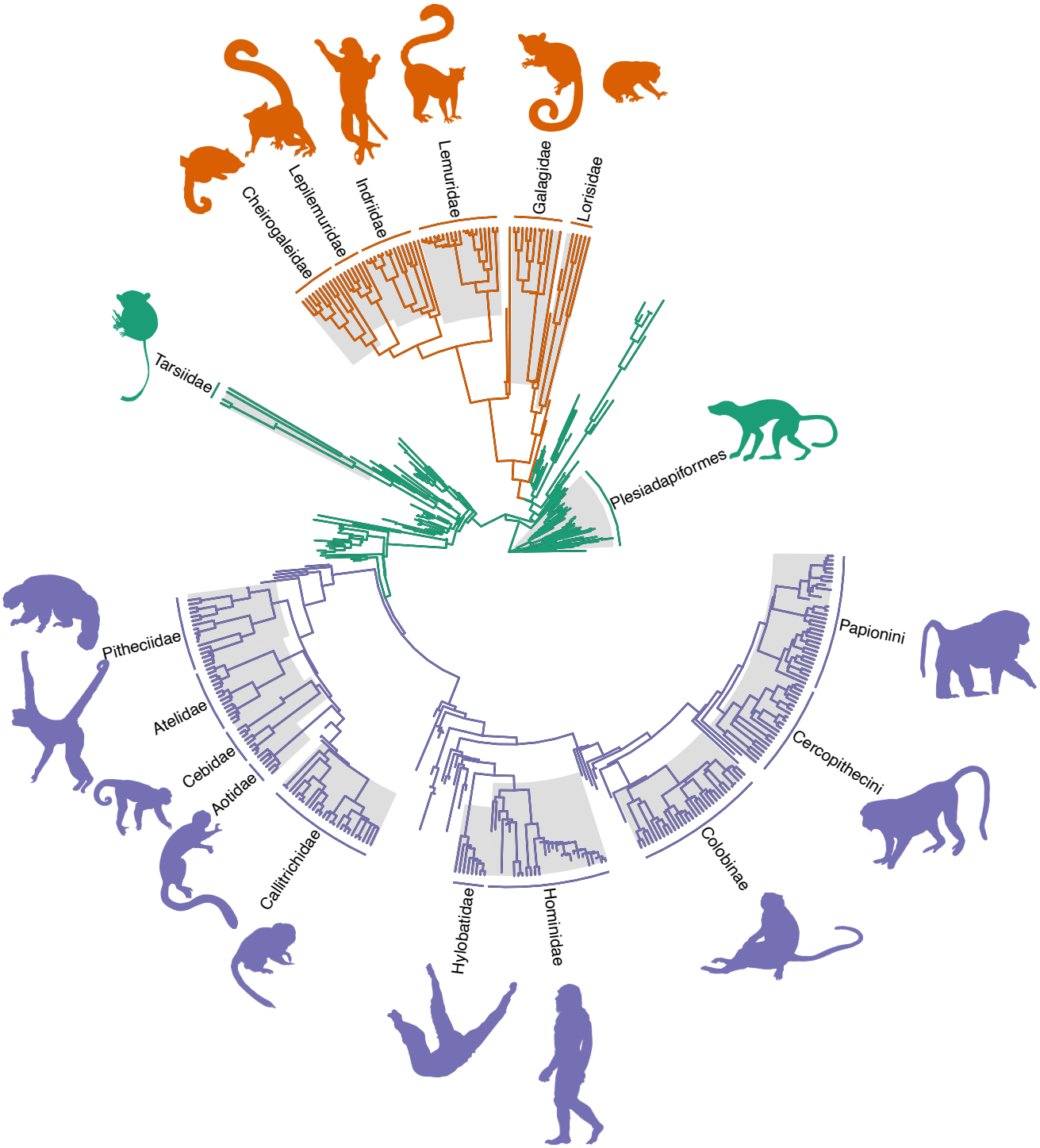

Fig. 1. Primate phylogenetic tree painted by the best regime combination found on the mixed model search for the individual molar areas. For areas and linear distances, the best model overall is a multi-regime BM, while for ICM ratios the best mixed model is a multi-regime OU (Table 1). However, for ICM ratios, single-regime microevolutionary models outperform all mixed models.

While primate molar teeth show compelling evidence for building the bridge between micro and macroevolution, it is possible that the application of the same framework in other biological systems might not produce similar results. First, molars are serially homologous units that are particularly insulated from environmental effects during development, resulting in a relatively simple ontogenetic

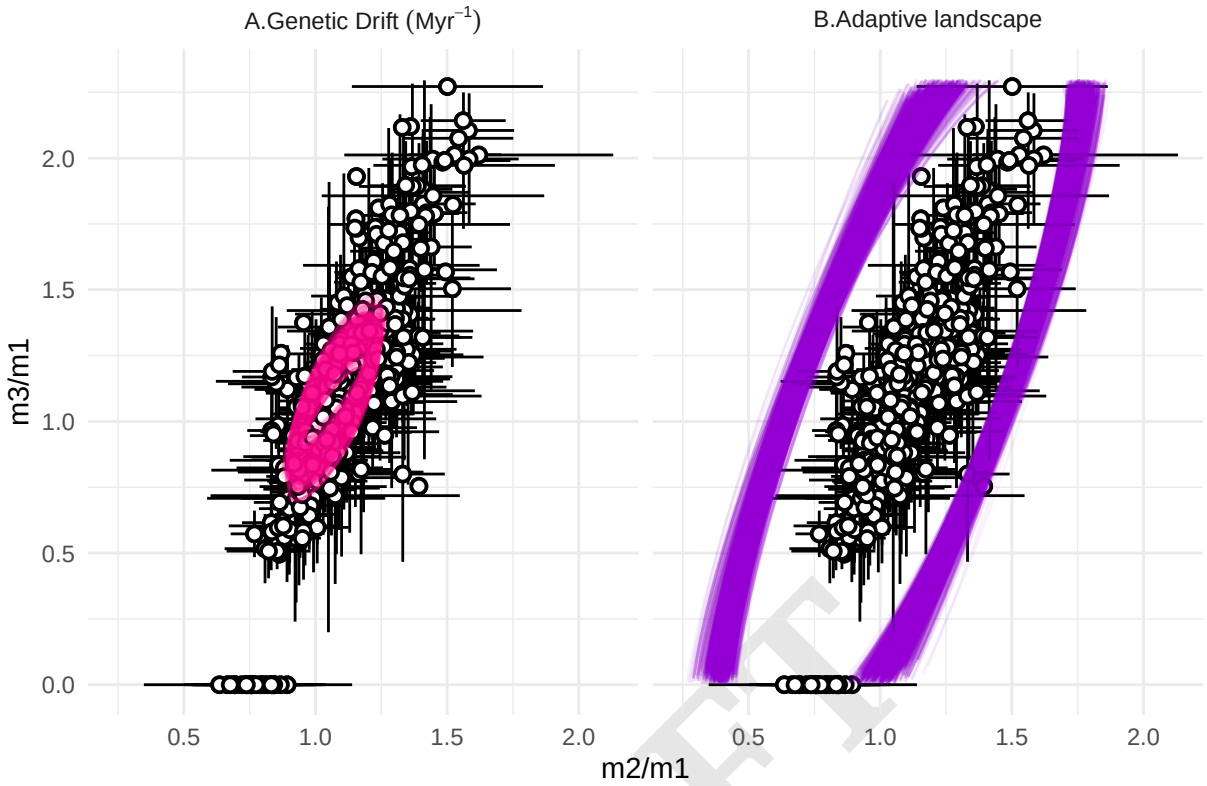

Fig. 2. Graphical representation of the best selected model for the ICM variables based on molar ratios m2/m1 and m3/m1. Dots are species averages, and horizontal and vertical lines depict ± 1.96 standard deviations. Ellipses are covariance matrices representing parameters of the best model. A. Stochastic rate matrix attributed to the amount of genetic drift introduced in the system every 1 myr. B. Individual adaptive landscape based on model estimates for the rate of adaptation towards the optima. Multiple ellipses were calculated from parameter value combinations that are sampled along the multi-dimensional likelihood contour 2 log-likelihoods away from the peak.

DRAFT

model (36). Second, various aspects of Primates' biology, both morphological and genetic, have been shown to conform to expectations of neutral evolution (20). And third, the availability of fossil teeth can cover much of the phenotypic discontinuities that could be identified as model heterogeneity. Combined, these factors might help explain why we found such a seamless transition between micro- and macroevolution. Nevertheless, even if the evolution of a phenotype does not conform to a specific microevolutionary model, the same models can be used as null-hypothesis, informative priors, and investigative tools for understanding phenotypic evolution. For example, recent studies have shown that deviations from null-microevolutionary models can be used to diagnose the action of directional selection in comparative data (15, 58), contrary to what was previously believed (20). This reinforces that model parameters estimated from macroevolutionary data can be meaningfully connected to expectations from microevolutionary processes. Thus, we hope that the framework and dataset provided here opens the door to the incorporation of strong biological assumptions in comparative analyses and facilitates the interrogation of the ultimate causes of macroevolutionary patterns.

Conclusions

To what degree microevolution can be extended to macroevolution is a central question in evolutionary biology (4). While there is little doubt that the fundamental causes at both levels are the same (*e.g.* selection, drift, mutation), efforts to model the connection have generally failed beyond qualitative alignment of patterns. When it comes to morphological evolution, the consensus has

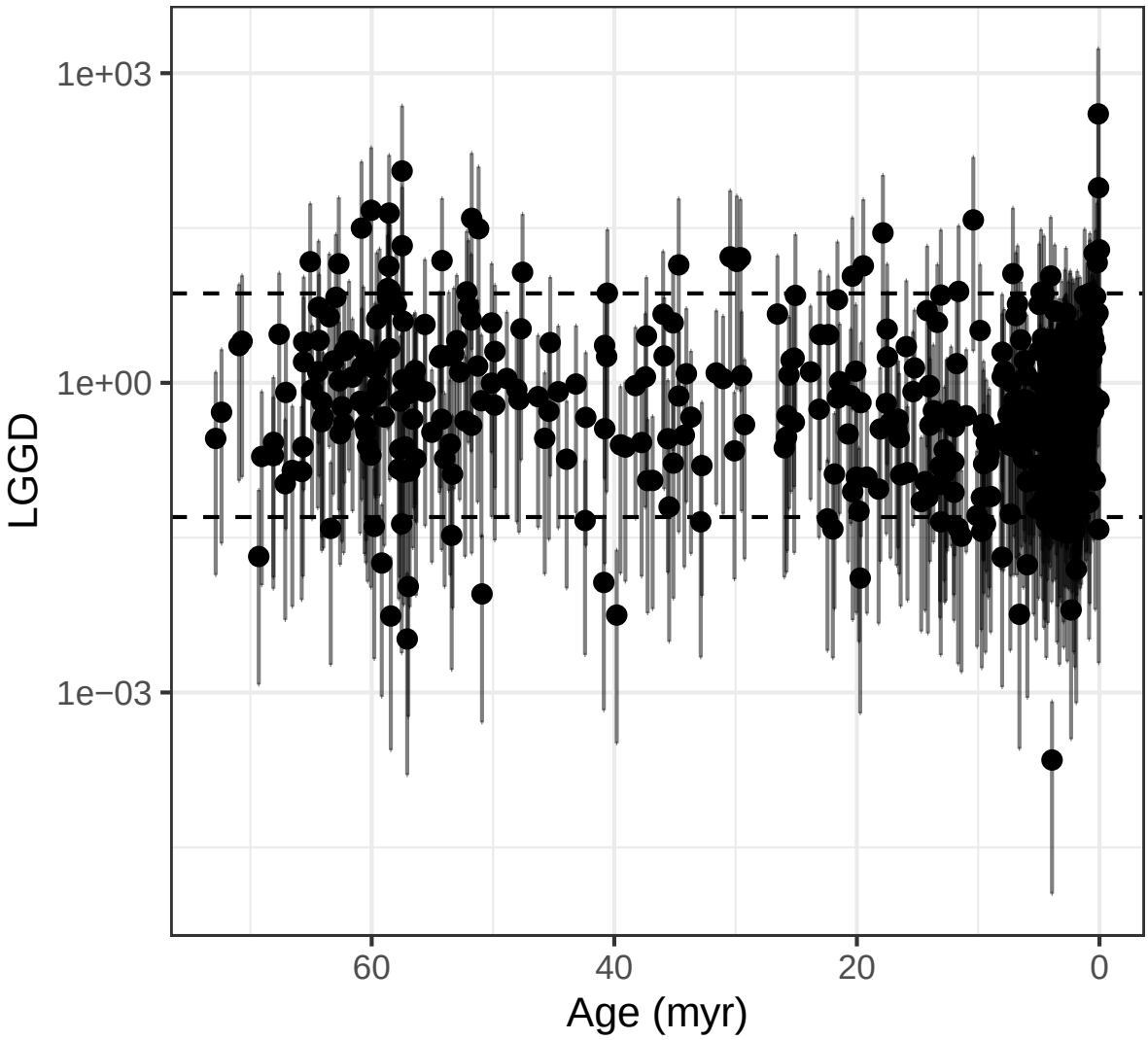

Fig. 3. Lande's Generalized Genetic Distance (LGGD) used to measure the node-specific rate of evolution throughout Primate divergence and diversification. Dashed lines represent the expected rates under genetic drift. For each node, a distribution of values were calculated by integrating over the variation in heritability, effective population size and generation time. Dots represent the median values and vertical lines at the 95% confidence interval.

been overwhelmingly to reject any straightforward connection between both levels, and pointed toward fundamental paradoxes in our understanding of the link between scales (6, 20). The results presented here reject this consensus. Even the relatively simple task of characterizing the multivariate dimensions of three molars poses a large number of choices for measurement. Our results suggest that biologically-informed quantification based on evo-devo maximally narrows the gap between both levels of analysis–and allow for the discovery of the underlying subspaces that both qualitatively and quantitatively align macroevolutionary patterns with microevolutionary processes.

Our investigation also provides a new framework in which developmental biology can be more fully incorporated into macroevolutionary modeling. It has long been considered that developmental biology was left out of the evolutionary synthesis (27–29), and indeed such data are rarely incorporated into comparative analyses. Recent efforts have had different degrees of success, with many pointing out how complexities of the ontogenetic systems can lead to core violations of the modern synthesis (27, 29, 32, 33, 40). By reframing the question of microevolutionary model adequacy into a problem of quantification of biological phenomena (38, 39), we show how evo-devo is essential for a fully

unified view in the context of the evolutionary synthesis.

Materials and Methods

Sample and morphometrics. We used the standard mesiodistal length (MD) and buccolingual breadth (BL) as basic descriptors of each molar. MD and BL were obtained for each tooth of the lower molar row (m1, m2 and m3). We obtained raw measurements from available datasets in the literature (46–48) and from newly measured museum specimens. For rare species, including fossil ones, we took measurements from images that were either published or were provided to us. All photos used had a scale and were digitized using the Fiji software (71). See the supplementary material for a full list of references and sources used for data collection. In total, we compiled a sample of 6558 individuals distributed among 480 species, divided between 232 extant and 248 extinct species. To evaluate the evolution of these traits on a phylogenetic framework, we used the most comprehensive phylogeny available that included both living and fossil primate species (51).

From this dataset we constructed three distinct morphospaces (Fig. S1). For our biologically naïve representation of tooth form, we used a "distance space" based on linear distances obtained from each tooth and an "area space" based on each tooth's occlusal area. For our evo-devo-informed space, we used the ratios of the second and third molars in relation to the third (m2/m1 and m3/m1, respectively), as defined by the inhibitory cascade model of molar development (36). We call this last morphospace the "ICM space". Measurement error was accounted for by calculating the standard deviation of each measurement for each species. When a species had a sample of n=1, we assigned a standard deviation equal to the pooled within-group standard deviation. This implies a very high measurement error for species known from single specimens, such as the case of many fossils. The degree of genetic association between traits was approximated both by the intraspecific pooled phenotypic covariance matrix P, and an independently derived additive genetic covariance matrix G obtained from a pedigreed *Papio hamadryas* baboon population (42, 43).

Phylogenetic comparative methods. To model morphological evolution, we used a maximum-likelihood (ML) model selection approach, which fits different Brownian-motion (BM) and Ornstein-Uhlenbeck (OU) models under a mixed Gaussian phylogenetic models (MGPM) framework (72). Under this framework, the evolution of a k-dimensional multivariate trait is modeled as an OU process as follows:

$$dx(t) = -H(x(t) - \theta(t))dt + \Sigma_x dW(t) \qquad [1]$$

where H is the kxk selective rate matrix, $x(t)$ is a k vector of trait values at time t, $\theta(t)$ is a k vector of each trait evolutionary optima at time t, Σ_x is the Cholesky factor of the kxk stochastic rate matrix Σ (sometimes called evolutionary rate matrix) and $W(t)$ denotes the k-dimensional standard Wiener process.

Under a strict quantitative genetics interpretation (73), the diagonal of H contains the rate of adaptation to the optima of each trait (α_k) and the off-diagonal measures the shape of co-selection among traits. Conversely, the diagonal of Σ contains the rate of evolution due to drift, with its off-diagonal elements containing the amount of coevolution due to genetic covariation. If H is a matrix of zeros, the model collapses into a multivariate BM model.

Under this microevolutionary perspective, Σ is not an entirely free parameter. Instead, if Σ is the genetic drift parameter, then it has to be proportional to the additive genetic covariance matrix G of those traits (74) as follows

$$\Sigma = G\frac{t_g}{Ne} \qquad [2]$$

DRAFT

where t_g is the time in generations and Ne is the effective population size. Because t_g and Ne, and even the size of G are hard to estimate at evolutionary time scales, some have argued for treating t_g/Ne as a nuisance parameter, reducing the investigation of drift at the macroevolutionary scale to a simple evaluation of the proportionality between Σ and G (56, 57, 59). Consistent with these suggestions, here we implement a series of proportionality models, or κ-models (25), in which Σ is set to be equal to a target matrix times a scaling factor κ. We used both the intraspecific pooled phenotypic covariance matrix P and G as target matrices. These models are implemented in the package PCMkappa (https://github.com/FabioLugar/PCMkappa).

Because the proportionality models are more tightly connected to a microevolutionary interpretation of the OU model, we call them "microevolutionary models". Full models (models where all parameters are estimated freely) are called "macroevolutionary models" because they do not have explicit microevolutionary assumptions.

We fitted two macroevolutionary BM and OU models and two microevolutionary models, using either P or G as a target matrix, for both BM and OU, totaling six global models (full BM and OU, $BM_{\Sigma\propto P}$, $BM_{\Sigma\propto G}$, $OU_{\Sigma\propto P}$, $OU_{\Sigma\propto G}$) for each morphospace. For the OU models, we investigated the confidence intervals of the parameters (see Supplementary Material) to evaluate if the model could be further reduced. Specifically, if the confidence interval of the off-diagonal elements of H overlapped with 0, another model was fit, setting H to be a diagonal matrix (72).

In addition, we performed a mixed Gaussian phylogenetic model search, which searches for the combination of regimes, models and model parameters that best fit the data (72). For both the mixed model search and model comparison, we used the Bayesian Information Criterion (BIC), which minimizes parameter inflation due to large samples and is most appropriate for our model-selection question (75) (i.e. asymptotically identifying the data-generating process as opposed to minimizing trait prediction error). For the mixed gaussian models, we only fit full BM and OU models, and no κ-model due to software restrictions. Therefore, the mixed models are also considered macroevolutionary models.

To ensure that the κ-models were compatible with microevolutionary processes, we constrained the κ parameter to be within the range of expected values under drift, as expressed in equation 2. Because Σ is given in the tree (myr) scale, we found approximations for t_g and of Ne for Primates to infer the expected scaling factor κ. t_g was estimated as $t_g = 1myr/g_t$, where g_t is the average generation time in years obtained from (53). Because we lack good estimates of g_t for fossil species, we used the phylogenetic average $\pm$ the standard deviation (SD) throughout the phylogeny. This was done by trimming the dataset to only the species with g_t data and obtaining the ancestral value and SD at the base through ML (76). For Ne we used 20,000-1,000,000 as the range of possible values consistent with the genomics estimates for multiple primate species and hypothetical common ancestors (54). While g_t and Ne are expected to vary over the tree, we assumed that the effect of this variation would be at least partially canceled out by the fact that these two quantities are generally inversely related to each other.

To evaluate the fitted model mechanistically under quantitative genetics theory, we generalized the equation for the adaptive landscape (17, 73) to the multivariate case as

$$\Omega = H^{-1/2} G H^{-1/2} - P \qquad [3]$$

Rates of evolution. Rates of evolution were used to evaluate if the evolutionary change conforms to the expectation of genetic drift. To calculate rates of evolution, we employed Lande's generalized genetic distance (LGGD, 74)

$$LGGD = \frac{N_e}{t_g} \Delta z^t \mathbf{G}^{-1} \Delta z \qquad [4]$$

where Δz is the phenotypic divergence calculated as the time-standardized phylogentic independent contrasts (PIC) for each node (15, 19). We produced a distribution of values for each node by altering values of G, N_e and t_g between the range defined above. Confidence intervals for the null-hypothesis of drift were generated from simulations based on equation 2 (15). Values that fall within the bounds of the null-distribution are

DRAFT

thought to conform to the expectation under genetic drift. Values that fall above or below are thought to be indicative of directional or stabilizing selection, respectively.

ACKNOWLEDGMENTS. We would like to thank Dr. Eric Delson and colleagues for access to the PRIMO dataset (48), Dr. Laurie Godfrey and Dr. Karen Samonds for the access to their Strepsirrhine molar data (47), Dr. Gustavo Burin for photographing specimens at the British Museum of Natural History, Dr. Guilherme Garbino for measuring specimens at the Museu de Zoologia João Moojen of the Universidade Federal de Viçosa, Anastasiya Kurylyuk and Dr. Rasoloarison M. Rodin for providing photographs of rare *Microcebus* specimens, and Marisa Surovy for providing access to the American Museum of Natural History specimens. FAM, JCU, VD, and AS were funded by NSF-DEB-1942717 to JCU.

1. T Dobzhansky, *Genetics and the Origin of Species.* (Columbia university press) No. 11, (1982).
2. MD de Santis, Misconceptions about historical sciences in evolutionary biology. *Evol. biology* **48**, 94–99 (2021).
3. SM Stanley, A theory of evolution above the species level. *Proc. Natl. Acad. Sci. United States Am.* **72**, 646–650 (1975).
4. SJ Gould, *The structure of evolutionary theory.* (Harvard University Press), (2002).
5. JC Uyeda, TF Hansen, SJ Arnold, J Pienaar, The million-year wait for macroevolutionary bursts. *Proc. Natl. Acad. Sci. United States Am.* **108**, 15908–15913 (2011).
6. D Houle, GH Bolstad, K van der Linde, TF Hansen, Mutation predicts 40 million years of fly wing evolution. *Nature* **548**, 447–450 (2017).
7. DH Erwin, Macroevolution is more than repeated rounds of microevolution. *Evol. & Dev.* **2**, 78–84 (2000).
8. M Hautmann, What is macroevolution? *Palaeontology* (2019).
9. R Lande, The dynamics of peak shifts and the pattern of morphological evolution. *Paleobiology* **12**, 343–354 (1986).
10. B Charlesworth, R Lande, M Slatkin, A neo-darwinian commentary on macroevolution. *Evolution* **36**, 474 (1982).
11. SJ Arnold, ME Pfrender, AG Jones, The adaptive landscape as a conceptual bridge between micro- and macroevolution. *Genetica* **112-113**, 9–32 (2001).
12. PD Polly, Developmental dynamics and g-matrices: Can morphometric spaces be used to model phenotypic evolution? *Evol. biology* **35**, 83–96 (2008).
13. TF Hansen, Macroevolutionary quantitative genetics? a comment on polly (2008). *Evol. Biol.* **35**, 182–185 (2008).
14. D Melo, A Porto, JM Cheverud, G Marroig, Modularity: genes, development and evolution. *Annu. review ecology, evolution, systematics* **47**, 463–486 (2016).
15. FA Machado, G Marroig, A Hubbe, The pre-eminent role of directional selection in generating extreme morphological change in glyptodonts (cingulata; xenarthra). *Proc. Royal Soc. B: Biol. Sci.* **289** (2022).
16. MW Pennell, LJ Harmon, An integrative view of phylogenetic comparative methods: connections to population genetics, community ecology, and paleobiology. *Annals New York Acad. Sci.* **1289**, 90–105 (2013).
17. TF Hansen, EP Martins, Translating between microevolutionary process and macroevolutionary patterns: the correlation structure of interspecific data. *Evolution* **50**, 1404–1417 (1996).
18. TF Hansen, Stabilizing selection and the comparative analysis of adaptation. *Evolution* **51**, 1341 (1997).
19. J Felsenstein, Phylogenies and quantitative characters. *Annu. review ecology systematics* **19**, 445–471 (1988).
20. M Lynch, The rate of morphological evolution in mammals from the standpoint of the neutral expectation. *The Am. Nat.* **136**, 727–741 (1990).
21. S Estes, SJ Arnold, Resolving the paradox of stasis: models with stabilizing selection explain evolutionary divergence on all timescales. *The american naturalist* **169**, 227–244 (2007).
22. TF Hansen, D Houle, Evolvability, stabilizing selection and the problem of stasis. *Phenotypic integration: Stud. ecology evolution complex phenotypes* p. 130 (2004).
23. GH Bolstad, et al., Genetic constraints predict evolutionary divergence in dalechampia blossoms. *Philos. Transactions Royal Soc. B: Biol. Sci.* **369**, 20130255 (2014).
24. JW McGlothlin, et al., Adaptive radiation along a deeply conserved genetic line of least resistance in anolis lizards. *Evol. letters* **2**, 310–322 (2018).
25. C Mongle, et al., Developmental processes mediate alignment of the micro- and macroevolution of primate molars. *Evolution* (In revision).
26. DW Thompson, DW Thompson, *On growth and form.* (Cambridge university press Cambridge) Vol. 2, (1942).
27. P Alberch, SJ Gould, GF Oster, DB Wake, Size and shape in ontogeny and phylogeny. *Paleobiology* **5**, 296–317 (1979).
28. P Alberch, Ontogenesis and morphological diversification. *Am. zoologist* **20**, 653–667 (1980).
29. SJ Gould, *Ontogeny and phylogeny.* (Belknap press), (1977).
30. TD Hether, PA Hohenlohe, Genetic regulatory network motifs constrain adaptation through curvature in the landscape of mutational (co)variance. *Evolution* **68**, 950–964 (2014).
31. JM Cheverud, Quantitative genetics and developmental constraints on evolution by selection. *J. Theor. Biol.* **110**, 155–171 (1984).
32. M Linde-Medina, R Diogo, Do correlation patterns reflect the role of development in morphological evolution? *Evol. biology* **41**, 494–502 (2014).
33. I Salazar-Ciudad, J Jernvall, A computational model of teeth and the developmental origins of morphological variation. *Nature* **464**, 583–586 (2010).
34. K Pearson, AG Davin, On the biometric constants of the human skull. *Biometrika* **16**, 328 (1924).
35. DM Raup, Geometric analysis of shell coiling: general problems. *J. paleontology* pp. 1178–1190 (1966).
36. KD Kavanagh, AR Evans, J Jernvall, Predicting evolutionary patterns of mammalian teeth from development. *Nature* **449**, 427–432 (2007).
37. V Alba, JE Carthew, RW Carthew, M Mani, Global constraints within the developmental program of the drosophila wing. *eLife* **10** (2021).
38. FL Bookstein, Measurement, explanation, and biology: Lessons from a long century. *Biol. theory* **4**, 6–20 (2009).
39. D Houle, C Pélabon, GP Wagner, TF Hansen, Measurement and meaning in biology. *The Q. Rev. Biol.* **86**, 3–34 (2011).
40. P Mitteroecker, The developmental basis of variational modularity: Insights from quantitative genetics, morphometrics, and developmental biology. *Evol. biology* **36**, 377–385 (2009).
41. JC Uyeda, DS Caetano, MW Pennell, Comparative analysis of principal components can be misleading. *Syst. Biol.* **64**, 677–689 (2015).
42. LJ Hlusko, ML Maas, MC Mahaney, Statistical genetics of molar cusp patterning in pedigreed baboons: implications for primate dental development and evolution. *J. Exp. Zool. Part B, Mol. Dev. Evol.* **302**, 268–283 (2004).
43. LJ Hlusko, RD Sage, MC Mahaney, Modularity in the mammalian dentition: mice and monkeys share a common dental genetic architecture. *J. Exp. Zool. Part B, Mol. Dev. Evol.* **316**, 21–49 (2011).
44. AM Hardin, Genetic correlations in the dental dimensions of saguinus fuscicollis. *Am. J. Phys. Anthropol.* **169**, 557–566 (2019).
45. AM Hardin, Genetic correlations in the rhesus macaque dentition. *J. Hum. Evol.* **148**, 102873 (2020).
46. JM Plavcan, Ph.D. thesis (Duke University) (1990).
47. LR Godfrey, KE Samonds, WL Jungers, MR Sutherland, Teeth, brains, and primate life histories. *Am. J. Phys. Anthropol. The Off. Publ. Am. Assoc. Phys. Anthropol.* **114**, 192–214 (2001).
48. E Delson, WE Harcourt-Smith, SR Frost, CA Norris, Databases, data access, and data sharing in paleoanthropology: first steps (2007).
49. V Bernal, PN Gonzalez, SI Perez, Developmental processes, evolvability, and dental diversification of new world monkeys. *Evol. Biol.* **40**, 532–541 (2013).
50. KE Carter, S Worthington, The evolution of anthropoid molar proportions. *BMC Evol. Biol.* **16**, 110 (2016).
51. AL Wisniewski, GT Lloyd, GJ Slater, Extant species fail to estimate ancestral geographical ranges at older nodes in primate phylogeny. *Proc. Royal Soc. B* **289**, 20212535 (2022).
52. LJ Revell, LJ Harmon, DC Collar, Phylogenetic signal, evolutionary process, and rate. *Syst. biology* **57**, 591–601 (2008).
53. M Pacifici, et al., Generation length for mammals. *Nat. Conserv.* **5**, 89 (2013).
54. M Brevet, N Lartillot, Reconstructing the history of variation in effective population size along phylogenies. *Genome Biol. Evol.* **13** (2021).
55. D Schluter, Adaptive radiation along genetic lines of least resistance. *Evolution* **50**, 1766 (1996).
56. G Marroig, JM Cheverud, Did natural selection or genetic drift produce the cranial diversification of neotropical monkeys? *The Am. Nat.* **163**, 417–428 (2004).
57. FA Machado, Selection and constraints in the ecomorphological adaptive evolution of the skull of living canidae (carnivora, mammalia). *The Am. Nat.* **196**, 197–215 (2020).
58. L Schroeder, N von Cramon-Taubadel, The evolution of hominoid cranial diversity: A quantitative genetic approach. *Evolution* **71**, 2634–2649 (2017).
59. RR Ackermann, JM Cheverud, Discerning evolutionary processes in patterns of tamarin (genus saguinus) craniofacial variation. *Am. J. Phys. Anthropol.* **117**, 260–271 (2002).
60. D Melo, G Marroig, Directional selection can drive the evolution of modularity in complex traits. *Proc. Natl. Acad. Sci. United States Am.* **112**, 470–475 (2015).
61. AG Jones, R Bürger, SJ Arnold, PA Hohenlohe, JC Uyeda, The effects of stochastic and episodic movement of the optimum on the evolution of the g-matrix and the response of the trait mean to selection. *J. Evol. Biol.* **25**, 2210–2231 (2012).

DRAFT

62. R Riedl, *Order in living organisms: a systems analysis of evolution*. (John Wiley & Sons), (1978).
63. RA Watson, GP Wagner, M Pavlicev, DM Weinreich, R Mills, The evolution of phenotypic correlations and "developmental memory". *Evolution* **68**, 1124–1138 (2014).
64. J Cheverud, The evolution of genetic correlation and developmental constraints in *Population genetics and evolution*. (Springer), pp. 94–101 (1988).
65. PD Polly, Development with a bite. *Nature* **449**, 413–414 (2007).
66. TJD Halliday, A Goswami, Testing the inhibitory cascade model in mesozoic and cenozoic mammaliaforms. *BMC Evol. Biol.* **13**, 79 (2013).
67. M Asahara, Unique inhibitory cascade pattern of molars in canids contributing to their potential to evolutionary plasticity of diet. *Ecol. Evol.* **3**, 278–285 (2013).
68. L Varela, PS Tambusso, RA Fariña, Unexpected inhibitory cascade in the molariforms of sloths (folivora, xenarthra): a case study in xenarthrans honouring gerhard storch's open-mindedness. *Frühförderung interdisziplinär* **76**, 1–16 (2020).
69. A Sadier, et al., Growth rate as a modulator of tooth patterning during adaptive radiations. *BioRxiv* (2021).
70. H Glowacka, GT Schwartz, A biomechanical perspective on molar emergence and primate life history. *Sci. Adv.* **7**, eabj0335 (2021).
71. J Schindelin, et al., Fiji: an open-source platform for biological-image analysis. *Nat. methods* **9**, 676–682 (2012).
72. V Mitov, K Bartoszek, T Stadler, Automatic generation of evolutionary hypotheses using mixed gaussian phylogenetic models. *Proc. Natl. Acad. Sci.* **116**, 16921–16926 (2019).
73. R Lande, Natural selection and random genetic drift in phenotypic evolution. *Evolution* **30**, 314 (1976).
74. R Lande, Quantitative genetic analysis of multivariate evolution, applied to brain:body size allometry. *Evolution* **33**, 402–416 (1979).
75. B Dennis, JM Ponciano, ML Taper, SR Lele, Errors in statistical inference under model misspecification: evidence, hypothesis testing, and AIC. *Front. ecology evolution* **7** (2019).
76. D Schluter, T Price, AØ Mooers, D Ludwig, Likelihood of ancestor states in adaptive radiation. *Evolution* **51**, 1699–1711 (1997).
77. G Marroig, J Cheverud, Size as a line of least resistance II: direct selection on size or correlated response due to constraints? *Evolution* **64**, 1470–1488 (2010).

DRAFT

Supplementary Materials

Contents

A Morphometrics **2**
- A Morphospaces . . . 2
- B G-matrix . . . 3

B Model comparison **5**
- A Distance space . . . 5
- B Area space . . . 6
- C ICM space . . . 6

C Confidence Intervals **7**

D Phylogenetic Half-lives **8**

E Disparity and phylogenetic signal **10**

F Regime-specific disparity **11**

G References used in data gathering **14**

H Supplementary references **19**

DRAFT

A. Morphometrics

A. Morphospaces. We used three morphospaces to test our hypothesis that evo-devo-informed quantification would provide a better bridge between micro and macroevolution. The first is based on the linear distances taken directly from the teeth, constituting a 6-dimensional space (“distance space”). The second morphospace is based on the occlusal areas of each molar, which were calculated using a rectangular approximation (65, 66), producing a 3-dimensional space (“area space”). These two spaces are considered naïve because they make no assumptions about underlying developmental processes. As a biologically informed space, we used the ICM description of the molar development (36), and constructed a morphospace based on the relation between the relative occlusal area of m2 and m3 in relation to m1 (m2/m1 and m3/m1, respectively), resulting in a 2-dimensional space ("ICM space"). Variables were log-transformed in both the trait and area datasets, but not in the ICM space.

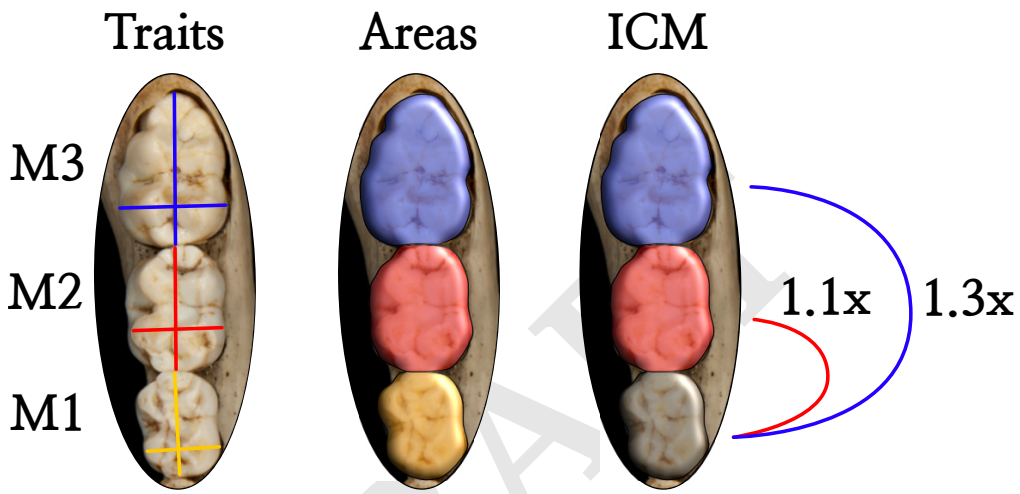

Fig. S1. Schematic representation of variables used to construct morphospaces. The trait-space was build on the mesiodistal length (MD, vertical) and buccolingual breadth (BL, horizontal) taken from each molar. The area-space was built by estimating the occlusal areas of each molar as the $A = MDxBL$. The ICM-space was built by calculating the relative area size for m2 and m3 in relation to m1.

DRAFT

An inspection of the the first two leading principal components of each morphospace (fig. S2) show that the naïve spaces are more patchy than the ICM space. Similarly, coloring species by the regime in fig. 1 suggests that groups diverge more and do not share similar trends of diversification on the naïve spaces. For the ICM space, though, groups overlap greatly and are more alignment in general trends.

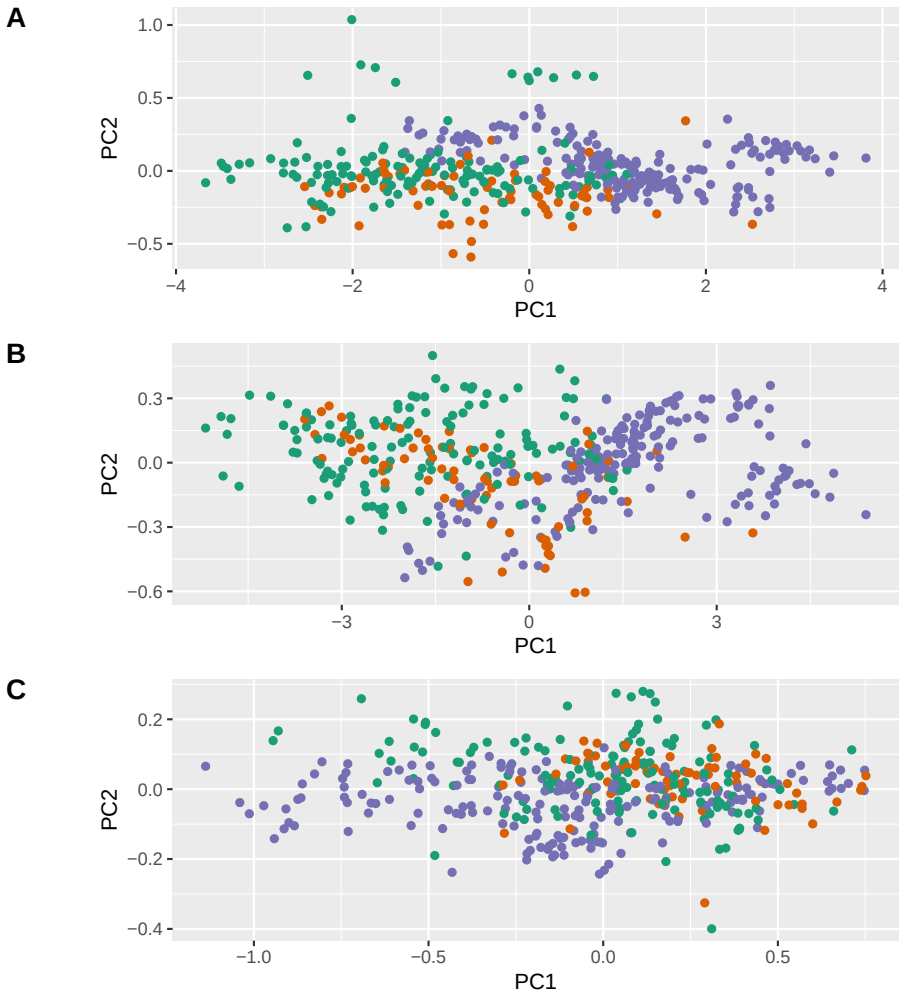

Fig. S2. Principal component analysis of the full-sample covariance matrix for the linear distances (A), areas (B) and ICM ratios (C) morphospaces. Dots represent species averages, and colors are the regimes depicted in fig. 1. Axes are not depicted to scale for convenience, so distances in the graph should not be considered representative of the metric of the underlying space.

B. G-matrix. To model the evolution of these traits under quantitative genetics models, we need an estimate of the additive genetic covariance matrix **G** for our molar traits. One common practice in comparative analysis is to use the pooled intraspecific phenotypic covariance matrix **P** as an approximation of **G** (15, 56, 57, 77). This is justified on the bases of the high similarity between **P** and **G** for morphological traits (25, 77). However, given that **P**s contain also non-genetic information, we also used **G** estimated from a pedigreed population of baboons as a direct model of the Primate **G** (42).

Because the G provided by (42) was estimated for the raw, untransformed BL and MD measures, we had to transform it in order to match our three morphospaces. We did this through a Monte-Carlo approach, in which we used the published G and population means to generate $n = 300$ samples of additive genetic effects. This number of samples was chosen to be compatible with effective sample sizes for the pedigreed population, and not over-represent the accuracy of the estimate (42). For the linear distance space, we took the generated genetic effects and log-transformed them. For the area space, we log-transformed the product of the effects for each tooth BL and MD. For the ICM space we took the product of the effects for each tooth BL and MD and divided the ones relative to m2 and m3 by m1. We then calculated the maximum-likelihood covariance matrix for the resulting effects for each space. This procedure was done 10,000 times, and the mean covariance matrix was taken as a point estimate of G for the lower-dimensionality morphospaces (area and ICM spaces).

To test the validity of this approach we compared the simulation results to the analytic approximation for covariance matrices of products of random variables. Specifically, we investigated if the covariance matrix obtained for the product of the additive effect for each tooth BL and MD (area space) are similar to what would be expected analytically as

$$\sigma^2_{xy} = \mu^2_x\sigma^2_y + \mu^2_y\sigma^2_x + (\sigma_{xy})^2 + 2\mu_x\mu_y\sigma_{xy} + \sigma^2_x\sigma^2_y \quad \text{[S1]}$$

$$\sigma^2_{xy,uv} = \mu_x\mu_u\sigma_{y,v} + \mu_x\mu_v\sigma_{y,u} + \mu_y\mu_u\sigma_{x,v} + \mu_y\mu_v\sigma_{y,u} + \sigma_{xu}\sigma_{yv}\sigma_{yu} \quad \text{[S2]}$$

where μ are means, σ^2 variances and σ are covariances for the random variables x, y, u and v (78). Variable pairs x:y and u:v are BL and MD variable pairs for each tooth. From these equations we were able to construct the covariance matrix for the area space on a cm^2 scale. This procedure was done only for this non-log area space as a proof-of-concept and to limit the number of assumptions necessary to derived log-scale and ratio spaces.

To compare analytical and Monte-Carlo estimates of G we first mean-scaled both matrices as follows:

$$\Sigma_\mu = \Sigma \oslash \bar{z}\bar{z}^t \quad \text{[S3]}$$

were Σ is the original covariance matrix, $\oslash$ is the element-wise product and $\bar{z}$ is a vector of means (13). We then calculated the absolute differences from each Monte-Carlo sample of these standardized matrices. Differences in the variances on these matrices are equal to the difference in coefficient of variation between matrices, and thus provide a dimensionless scale of comparison.

The results shows that matrices are extremely similar, with a slight bias for covariances being higher on the Monte Carlo samples (fig. S3). Despite this, all absolute differences are very small (< 0.002), suggesting that differences are negligible. A matrix correlation analysis reinforced this interpretation, showing values > 0.97 for all samples. Together, these results suggests that the Monte Carlo estimates are a reliable approximation for the covariance on lower dimensionalities.

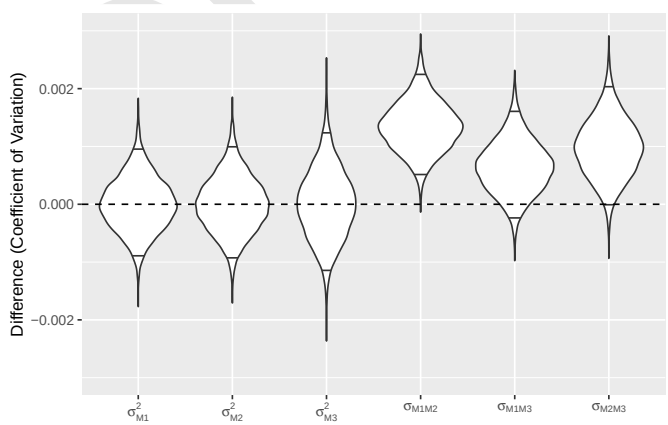

Fig. S3. Differences between the Monte Carlo sampling approach for generating covariances for areas and the analytical approximation. Horizontal lines within violins highlights the 95% interval for each matrix cell.

B. Model comparison

We performed model comparison under the maximum likelihood framework of the Phylogenetic mixed Gaussian models (72),(79). This framework has some desirable features. First, it incorporates both measurement errors and missing data during the model fitting procedure. The latter is especially important in our case due to the abundance of fossil taxa in our sample and the presence of species lacking m3s, such as callitrichines and the fossil *Xenothrix mcgregori*. Second, it takes into account process heterogeneity along the tree, allowing regimes to be under different kinds of models and parameter combinations. Lastly, the parameters of the fitted model can be interpreted under quantitative genetics theory in terms of genetic drift and stabilizing selection (18).

To test our hypothesis, we fit global models that included some microevolutionary assumptions (κ-models) and some that did not. Evidence supporting κ-models could then be seen as evidence for a microevolutionary interpretation of the data. For each morphometric space, we fitted regular BM and OU models, as well as two κ versions of these models. For these models, the rate matrix Σ was set to be proportional to either P or G. We also performed mixed model heuristic searches, which try to find the best regime combination for a given tree, allowing for regimes to be under different model types (BM or OU). For each space, we conducted 10 searches and recorded the result with the lowest BIC. Lastly, in addition to the heuristic result, we tested mixed models with pre-determinate regime shifts base on Fig. 1 which is the best result for the area morphospace. This regime was chosen as a common point of reference to compare the effect of model and parameter heterogeneity on the fitting process.

A. Distance space. For the distance space only 6 out of 10 heuristic searches converged. Nevertheless, they all produced better BIC values than any global model (table S1). The best model (Search 5) was a multi-rate BM model, with two regimes, one for Simiiformes and one for the remaining of the tree (Fig.S4A). This model deviates from the best model chosen to represent the rate heterogeneity on the other spaces by essentially fusing the ancestral and the Strepsirrhini regimes into one (Fig. 1). In terms of model parameters, this model performed similarly as the tree-regime one in the sense that the ancestral regime had higher rates of evolution than the Simiiformes one (see below fig 3).

Despite the best model being different than the one described in the main text, Search 4 produced a regime combination that was essentially identical to the one for area (Fig. S4B). Even though the BIC was worse than the best model, this run performed better than any of the global models and is therefore adequate to highlight how this morphospace privileges more heterogeneous models instead of global ones.

Table S1. Comparison of models of the linear distance morphospace fit through Maximum Likelihood.

Model [a]	k [b]	logLik [c]	BIC [d]
BM	27	2585.03	-5112.72
OU	54	2684.57	-5247.16
$BM_{\Sigma \propto P}$	7	2108.57	-4202.91
$OU_{\Sigma \propto P}$	34	2174.45	-4275.55
$BM_{\Sigma \propto G}$	7	1480.63	-2947.02
$OU_{\Sigma \propto G}$	34	1510.57	-2947.79
Search 1	78	2788.91	-5391.08
Search 2	51	2796.77	-5479.14
Search 3	97	2868.67	-5493.57
Search 4	74	2823.03	-5470.65
Search 5	51	2878.96	**-5643.53**
Search 6	78	2820.77	-5454.80

[a] Model type; either global BM or OU (full or κ models) or a search run of mixed model.

[b] Number of model parameters.

[c] Log-likelihood of the model.

[d] Bayesian Information Criterion used for model comparison. Bold represents the best models, while underline represents the ones with BIC 2 units away from the best model.

DRAFT

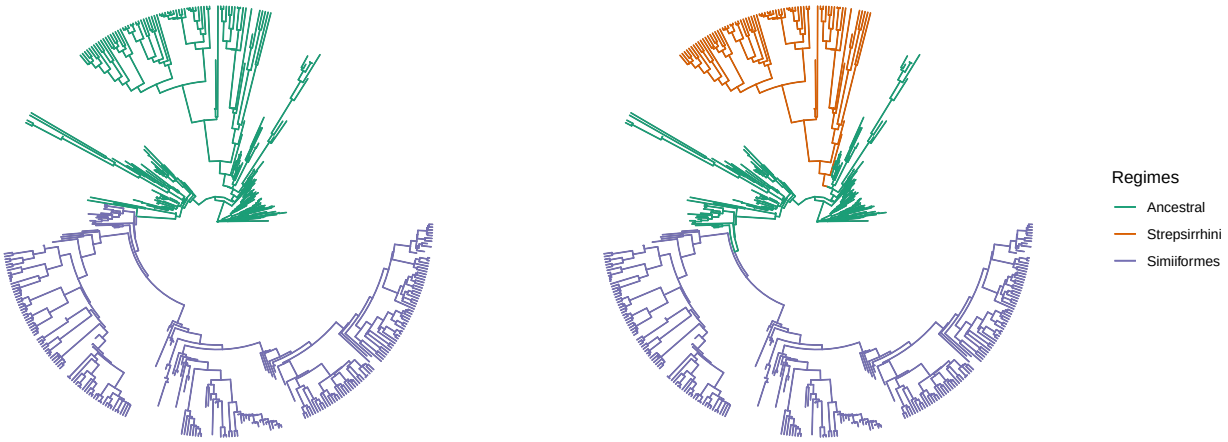

Fig. S4. Regimes for different runs of the heuristic search. A- Best model (Search 5). B- Model compatible with the best model for areas (Fig. 1)

B. Area space. For the area space, 9 out of the 10 heuristic searches converged. The best mixed model (Search 7) and the best overall model was a multi-rate BM model with three regimes, as described in the main text (Fig. 1).

C. ICM space. For the ICM space, all 10 heuristic searches converged. From these, four runs produced the same result as the global OU model (table S3), suggesting an absence of model shifts for this space. The global fits show that both OU and BM models are equally good fits to the data and that the addition of the microevolutionary assumption of proportionality between Σ and G for the global OU model produces a slightly superior model ($\mathrm{OU}_{\Sigma\propto G}$). Although all three models seem to provide a good fit to the data, the investigation of confidence intervals for parameters of the OU models shows that the confidence interval of the off-diagonal element of H overlaps with zero (tables S6,S7), suggesting that this parameter can be excluded from the model (see below).

A model that omits the off-diagonal elements of H is implemented as a default model in the PCMfit package (72). We chose not to include those models initially because our data is rich enough to estimate parameters from even fairly complex models. Instead, we chose to fit the most complex model and perform *post-hoc* model simplification. Using a κ-OU model with a diagonal H produces a model with vastly superior BIC ($\mathrm{OU}^{d}_{\Sigma\propto G}$). The removal of the off-diagonal elements of H did not change significantly the parameter estimates (table S9,S8). Lastly, although OU^{d} and $\mathrm{OU}^{d}_{\Sigma\propto G}$ had similar BICs, the confidence interval for all common parameters showed great overlap, suggesting that both models are equivalent. Furthermore, the $\mathrm{OU}^{d}_{\Sigma\propto G}$ model had tighter confidence intervals, fewer number of parameters and a slightly larger BIC. For these reasons, we chose this as the best model for our data.

DRAFT

Table S2. Comparison of models of the area morphospace fit through Maximum Likelihood.

Model [a]	k [b]	logLik [c]	BIC [d]
BM	9	415.80	-813.21
OU	18	413.98	-790.47
$BM_{\Sigma \propto P}$	4	92.39	-176.70
$OU_{\Sigma \propto P}$	13	275.16	-523.54
$BM_{\Sigma \propto G}$	4	74.41	-140.74
$OU_{\Sigma \propto G}$	13	258.02	-489.26
Search 1	10	413.61	-806.75
Search 2	10	414.98	-809.48
Search 3	19	420.25	-800.85
Search 4	10	415.85	-811.23
Search 5	18	434.43	-831.37
Search 6	26	469.34	-883.58
Search 7	26	471.42	**-887.74**
Search 8	10	415.17	-809.87
Search 9	27	448.71	-840.08

[a] Model type; either global BM or OU (full or κ models) or a search run of mixed model.

[b] Number of model parameters.

[c] Log-likelihood of the model.

[d] Bayesian Information Criterion used for model comparison. Bold represents the best models, while underline represents the ones with BIC 2 units away from the best model.

DRAFT

C. Confidence Intervals

Confidence intervals for model parameters and derived statistics were obtained by exploring the likelihood surface and getting parameter combinations from models that were 2 log-likelihood units away from the peak. This was done using the "dentist" package (https://github.com/bomeara/dentist), which allows the exploration of the likelihood surface by "denting" of the surface- setting the region around the peak to have extremely low likelihoods and sampling on the resulting contour around the dented peak. We used 10,000 steps to sample the likelihood surface and obtain confidence intervals simultaneously for all parameters for models fit on the ICM morphospace.

For the OU and $OU_{\Sigma \propto G}$ models, the off-diagonal elements of the H matrix ($H_{1,2}$) have confidence intervals that overlap with 0, suggesting that this parameter can be omitted from the model (table S6, S7). The removal of the $H_{1,2}$ from the model did not change substantially parameter estimates (table S8, S9), nor did it reduce the likelihoods of the models, improving BIC scores (table S3). All models showed a great overlap in the common parameters (table S6–S9). This is also true for the reconstructed Σ matrix for the *kappa* models. Specifically, for $OU^{d}_{\Sigma \propto G}$, Σ confidence intervals are $\Sigma_{1,1} = 0.0243 - 0.0276$, $\Sigma_{1,2} = 0.0324 - 0.0368$ and $\Sigma_{2,2} = 0.0666 - 0.0756$, placing them within the expected for the $OU_{\Sigma \propto G}$ model.

Table S3. Comparison of models of the ICM morphospace fit through Maximum Likelihood.

Model [a]	k [b]	logLik [c]	BIC [d]
BM	5	589.16	-1147.46
OU	10	604.53	-1147.33
OU^d	9	604.56	<u>-1153.55</u>
BM$_{\Sigma \propto P}$	3	538.31	-1058.10
OU$_{\Sigma \propto P}$	8	584.68	-1119.98
BM$_{\Sigma \propto G}$	3	575.69	-1132.86
OU$_{\Sigma \propto G}$	8	598.96	-1148.53
OU$^d_{\Sigma \propto G}$	7	598.54	**-1153.86**
Three-regime OU	26	597.35	-1034.18
Search 1	10	604.56	-1147.37
Search 2	15	618.60	-1144.59
Search 3	15	618.56	-1144.52
Search 4	15	617.78	-1142.95
Search 5	10	604.55	-1147.37
Search 6	15	617.80	-1142.99
Search 7	10	604.56	-1147.37
Search 8	6	589.16	-1141.28
Search 9	10	604.55	-1147.36
Search 10	15	617.80	-1143.00

[a] Model type; either global BM or OU (full or κ models) or a search run of mixed model.
[b] Number of model parameters.
[c] Log-likelihood of the model.
[d] Bayesian Information Criterion used for model comparison. Bold represents the best models, while underline represents the ones with BIC 2 units away from the best model.

Table S4. Confidence interval for the BM model.

	best	lower CI	upper CI	lowest examined	highest examined
$X0_1$ [a]	1.086	0.993	1.184	0.801	1.200
$X0_2$ [a]	1.184	1.003	1.364	0.801	1.599
$\Sigma_{1,1}$ [b]	0.018	0.016	0.020	0.010	0.499
$\Sigma_{1,2}$ [b]	0.030	0.026	0.032	0.010	0.498
$\Sigma_{2,2}$ [b]	0.071	0.065	0.077	0.010	0.497

[a] Ancestral state at the root
[b] Entries of the rate matrix.

DRAFT

D. Phylogenetic Half-lives

The investigation of the adaptive landscape implied by the best model shows a corridor-like topography (Fig. 2), suggesting that selection is relaxed along the activation-inhibition axis and intensified against deviations from the ICM. To further verify this without assuming a microevolutionary model, we calculated the phylogenetic half-lives ($t_{1/2}$) along the activation-inhibition gradient and the deviations from the ICM. $t_{1/2}$ measures the time it takes for the phenotype to move halfway in the direction of the optimum and is calculated as

$$t_{1/2} = ln(2)/\alpha \qquad \text{[S4]}$$

with α being the rate of adaptation for each trait given by the diagonal of the H matrix (18). Because H is given as a function of the original traits (m2/m1 and m3/m1) we have to perform a rotation of the original matrix into the eigenvectors of the adaptive landscape as

$$H^r = V^t H V \qquad \text{[S5]}$$

Table S5. Confidence interval for the BM$_{\Sigma \propto G}$ model.

	best	lower CI	upper CI	lowest examined	highest examined
$X0_1$ [a]	1.090	0.983	1.195	0.800	1.200
$X0_2$ [b]	1.182	1.005	1.348	0.800	1.593
κ [b]	0.361	0.317	0.413	0.102	0.899

[a] Ancestral state at the root

[b] Proportionality constant between the target matrix (**G**-matrix) and Σ.

Table S6. Confidence interval for the OU model.

	best	lower CI	upper CI	lowest examined	highest examined
$X0_1$ [a]	1.132	1.008	1.200	0.801	1.200
$X0_2$ [a]	1.306	1.075	1.466	0.804	1.597
$H_{1,1}$ [b]	0.034	0.025	0.043	0.010	0.498
$H_{1,2}$ [b]	-0.214	-0.485	0.473	-0.490	0.498
$H_{2,2}$ [b]	0.031	0.021	0.040	0.010	0.498
θ_1 [c]	1.064	1.012	1.115	0.808	1.198
θ_2 [c]	1.066	0.971	1.175	0.801	1.593
$\Sigma_{1,1}$ [d]	0.022	0.020	0.025	0.010	0.495
$\Sigma_{1,2}$ [d]	0.034	0.030	0.036	0.010	0.500
$\Sigma_{2,2}$ [d]	0.080	0.074	0.086	0.010	0.498

[a] Ancestral state at the root

[b] Entries of the **H**-matrix

[c] Multivariate optima

[d] Entries of the rate matrix

DRAFT

were V are the eigenvectors of Ω (see equation 3). $t_{1/2}$ were calculated integrating over the confidence limits of parameters. In addition to the rotated space, we also calculated $t_{1/2}$ on the original space. This was done to evaluate an additional hypothesis of the ICM process that m3s, because they develop last, are under less intense stabilizing selection (25).

The results for molar ratios are in line with this prediction, as the half-life for m3/m1 is considerably larger than for m2/m1, suggesting a stronger selection on the latter than in the former (fig S5). For the components of the ICM, results are compatible with the expected for a corridor-like adaptive landscape, with half-lives along the activation-inhibition gradient being higher than on the one for deviations from the ICM (fig S5). This suggests that selection against deviations from ICM is far stronger than the ones along the activation-inhibition gradient, allowing the near-neutral evolution within the adaptive corridor. An inspection of the evolutionary trait-grams of these variables reinforces this idea, as deviations from the ICM are more tightly confined around the optima, and evolution along the activation-inhibition gradient seems greater in amplitude (fig S6).

Table S7. Confidence interval for the OU$_{\Sigma \propto G}$ model

	best	lower CI	upper CI	lowest examined	highest examined
$X0_1$ [a]	1.097	0.966	1.192	0.800	1.199
$X0_2$ [a]	1.232	1.031	1.376	0.802	1.599
κ [b]	0.486	0.416	0.553	0.101	0.894
$H_{1,1}$ [c]	0.049	0.037	0.057	0.010	0.499
$H_{1,2}$ [c]	0.226	-0.352	0.469	-0.497	0.500
$H_{2,2}$ [c]	0.024	0.013	0.035	0.010	0.499
θ_1 [d]	1.066	1.027	1.106	0.800	1.198
θ_2 [d]	1.058	0.885	1.175	0.802	1.597

[a] Ancestral state at the root
[b] Proportionality constant between the target matrix (**G**-matrix) and Σ.
[c] Entries of the **H**-matrix
[d] Multivariate optima

Table S8. Confidence interval for the OU^d model

	best	lower CI	upper CI	lowest examined	highest examined
$X0_1$ [a]	1.102	1.012	1.192	0.801	1.199
$X0_2$ [a]	1.248	1.068	1.428	0.800	1.592
$H_{1,1}$ [b]	0.036	0.025	0.043	0.010	0.499
$H_{2,2}$ [b]	0.031	0.019	0.039	0.010	0.499
θ_1 [c]	1.066	1.016	1.112	0.801	1.200
θ_2 [c]	1.073	0.969	1.211	0.808	1.585
$\Sigma_{1,1}$ [d]	0.022	0.020	0.025	0.010	0.498
$\Sigma_{1,2}$ [c]	0.033	0.030	0.036	0.010	0.499
$\Sigma_{2,2}$ [c]	0.079	0.073	0.084	0.010	0.499

[a] Ancestral state at the root
[b] Entries of the **H**-matrix
[c] Multivariate optima
[d] Entries of the rate matrix

DRAFT

E. Disparity and phylogenetic signal

To illustrate the effect of stabilizing selection on both overall disparities in the sample and phylogenetic signal, we employed a simulation approach. We generated tip data using the phylogenetic tree and the best evolutionary model in two situations. In one, we used the whole model to produce data under an OU model; in another, we set the H matrix to be 0, producing a BM model with the same rate parameters as the OU model. For each model, we generated 1,000 datasets, and for each of these datasets, we extracted the overall disparity and the phylogenetic signal. The disparity was calculated simply as the sum of variances in the tip data, as a measure of overall morphospace occupancy (80). For Phylogenetic signal, we employed the multivariate version of Blomberg's K (81, 82). Results from the simulations show the expected pattern, with the BM model showing higher disparity and phylogenetic signal than the OU model (Fig. S7).

Table S9. Confidence interval for the $\mathrm{OU}^{d}_{\Sigma \propto G}$ model.

	best	lower CI	upper CI	lowest examined	highest examined
$X0_1$ [a]	1.107	0.963	1.190	0.800	1.200
$X0_2$ [a]	1.232	1.036	1.393	0.800	1.598
κ [b]	0.484	0.416	0.536	0.101	0.900
$H_{1,1}$ [c]	0.044	0.034	0.050	0.010	0.498
$H_{1,2}$ [c]	0.025	0.013	0.037	0.010	0.495
θ_1 [d]	1.066	1.029	1.109	0.800	1.200
θ_2 [d]	1.063	0.917	1.209	0.802	1.594

[a] Ancestral state at the root

[b] Proportionality constant between the target matrix (**G**-matrix) and Σ.

[c] Entries of the **H**-matrix

[d] Multivariate optima

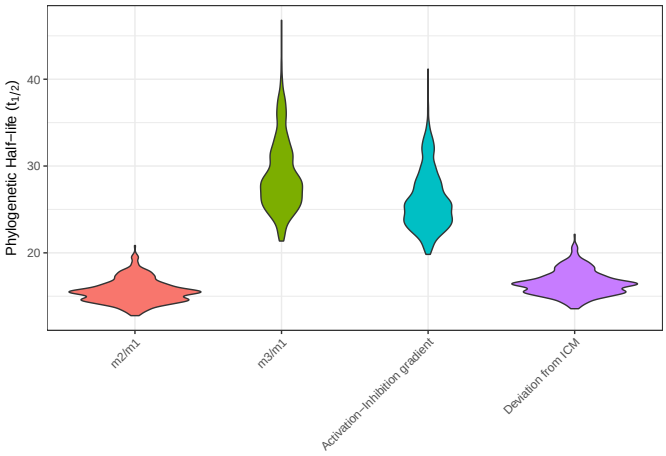

Fig. S5. Phylogenetic half life for ICM ratios (m2/m1 and m3/m1) and components of the ICM model (Activation-Inhibition gradient and deviations from the ICM).

F. Regime-specific disparity

To compare the disparity-generating potential of different regimes of the mixed-model depicted in Fig. 1, we employed a simulation approach. Specifically, we took each model for each regime and simulated phenotypic evolution according to that model on a star-phylogeny of equal size as the full phylogeny. This was done to standardize differences in tree-structure, species sample size and model differences (BM or OU) between regimes. Simulations were performed 100 times, and for each run we computed the disparity of the simulated tip data. This was done for the three-regime model for each morphospace. Higher and lower values of disparity are indicative of a less or more constrained evolution, respectively. Results show that, for all spaces, the ancestral regime is less constrained than the Strepsirrhini and Simiiform regimes (Fig. S8). For areas and distances, the difference between the ancestral and derived regimes disparity is greater than for the ICM morphospace, with Simiiform showing a higher disparity than Strepsirrhini.

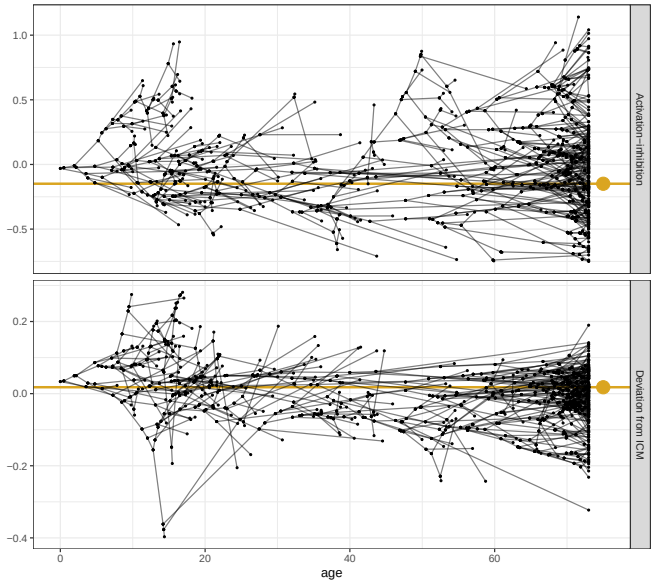

Fig. S6. Traitgrams of the components of the ICM for primates. Black lines represents the phylogeny mapped to measured trait values (black points) and golden lines and dots represents each trait optimum.

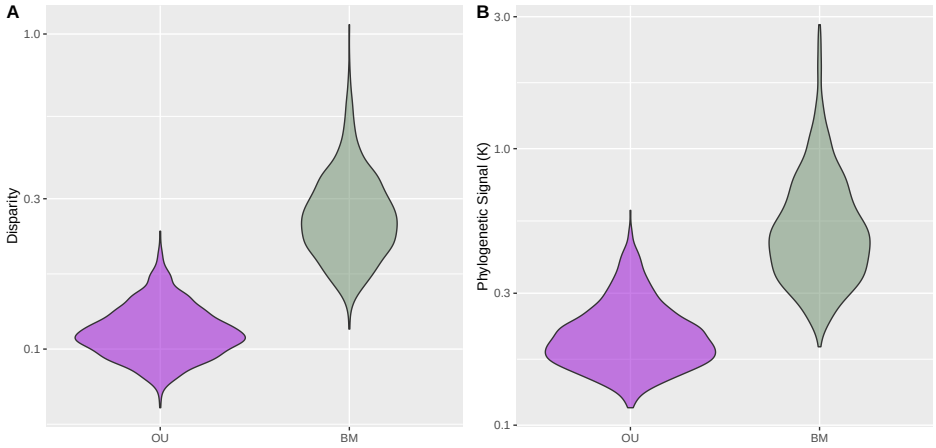

Fig. S7. Simulated disparity (A) and phylogenetic signal (B) by assuming the best model (OU) or a brownian motion (BM) model with the same rate parameters as the best OU model.

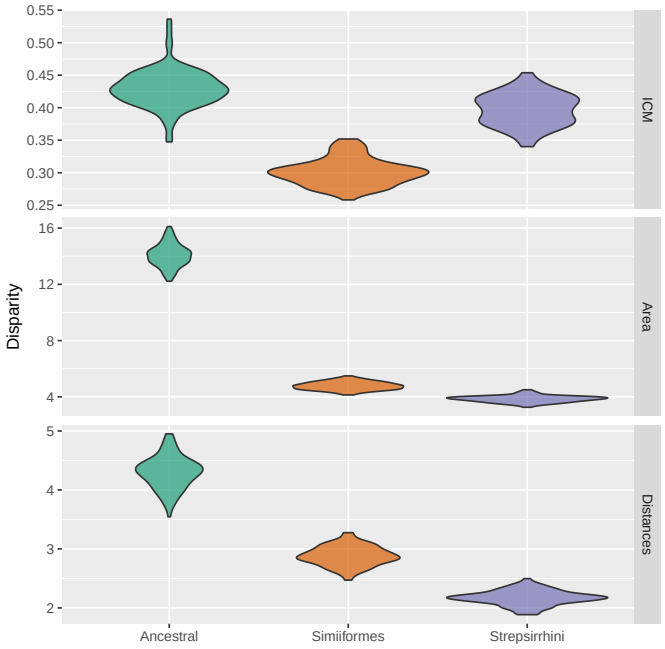

Fig. S8. Simulated regime-specific disparities for Three-regime model on morphospace.

G. References used in data gathering

Abbazzi, L., Fanfani, F., Ferretti, M. P., Rook, L., Cattani, L., Masini, F., ... and Tozzi, C. (2000). New human remains of archaic Homo sapiens and lower palaeolithic industries from Visogliano (Duino Aurisina, Trieste, Italy). Journal of Archaeological Science, 27(12), 1173-1186.

Alba, D. M. (2012). Fossil apes from the vallès-penedès basin. Evolutionary Anthropology: Issues, News, and Reviews, 21(6), 254-269.

Alba, D. M., Almécija, S., Casanovas-Vilar, I., Méndez, J. M., and Moyà-Solà, S. (2012). A partial skeleton of the fossil great ape Hispanopithecus laietanus from Can Feu and the mosaic evolution of crown-hominoid positional behaviors. PLoS One, 7(6), e39617.

Alba, D. M., Casanovas-Vilar, I., Almécija, S., Robles, J. M., Arias-Martorell, J., and Moyà-Solà, S. (2012). New dental remains of Hispanopithecus laietanus (Primates: Hominidae) from Can Llobateres 1 and the taxonomy of Late Miocene hominoids from the Vallès-Penedès Basin (NE Iberian Peninsula). Journal of human evolution, 63(1), 231-246.

Alba, D. M., Fortuny, J., de los Ríos, M. P., Zanolli, C., Almécija, S., Casanovas-Vilar, I., ... and Moyà-Solà, S. (2013). New dental remains of Anoiapithecus and the first appearance datum of hominoids in the Iberian Peninsula. Journal of human evolution, 65(5), 573-584.

Alba, D. M., Moyà-Solà, S., Malgosa, A., Casanovas-Vilar, I., Robles, J. M., Almécija, S., ... and Mengual, J. V. B. (2010). A new species of Pliopithecus Gervais, 1849 (Primates: Pliopithecidae) from the Middle Miocene (MN8) of Abocador de Can Mata (els Hostalets de Pierola, Catalonia, Spain). American Journal of Physical Anthropology: The Official Publication of the American Association of Physical Anthropologists, 141(1), 52-75.

Alba, D. M., Moyà-Solà, S., Robles, J. M., and Galindo, J. (2012). Brief communication: The oldest pliopithecid record in the Iberian Peninsula based on new material from the Vallès-Penedès Basin. American Journal of Physical Anthropology, 147(1), 135-140.

Andrews, P. (1970). Two new fossil primates from the Lower Miocene of Kenya. Nature, 228(5271), 537-540.

Andrews, P. (1974). New species of Dryopithecus from Kenya. Nature, 249(5453), 188-190.

Anthony, M. R., and Kay, R. F. (1993). Tooth form and diet in ateline and alouattine primates: reflections on the comparative method. American Journal of Science, 293(A), 356.

Asfaw, B., White, T., Lovejoy, O., Latimer, B., Simpson, S., and Suwa, G. (1999). Australopithecus garhi: a new species of early hominid from Ethiopia. Science, 284(5414), 629-635.

Atwater, A. L. (2017). New Middle Eocene Omomyines (Primates, Haplorhini) from the Friars Formation of San Diego County, Southern California (Doctoral dissertation).

Atwater, A. L., and Kirk, E. C. (2018). New middle Eocene omomyines (Primates, Haplorhini) from San Diego County, California. Journal of human evolution, 124, 7-24.

Bacon, A. M., Demeter, F., Schuster, M., Long, V. T., Thuy, N. K., Antoine, P. O., ... and Huong, N. M. (2004). The Pleistocene Ma U'Oi cave, northern Vietnam: palaeontology, sedimentology and palaeoenvironments. Geobios, 37(3), 305-314.

Bajpai, S., Kay, R. F., Williams, B. A., Das, D. P., Kapur, V. V., and Tiwari, B. N. (2008). The oldest Asian record of Anthropoidea. Proceedings of the National Academy of Sciences, 105(32), 11093-11098.

Barry, J. C., Jacobs, L. L., and Kelley, J. (1986). An early middle Miocene catarrhine from Pakistan with comments on the dispersal of catarrhines into Eurasia. Journal of Human Evolution, 15(6), 501-508.

Beard, K. C. (2000). A new species of Carpocristes (Mammalia: Primatomorpha) from the middle Tiffanian of the Bison Basin, Wyoming, with notes on carpolestid phylogeny. Annals of Carnegie Museum, 69(3), 195-208.

Beard, K. C., Jones, M. F., Thurber, N. A., and Sanisidro, O. (2019). Systematics and paleobiology of Chiromyoides (Mammalia, Plesiadapidae) from the upper Paleocene of western North America and western Europe. Journal of Vertebrate Paleontology, 39(6), e1730389.

Beard, K. C., Marivaux, L., Chaimanee, Y., Jaeger, J. J., Marandat, B., Tafforeau, P., ... and Kyaw, A. A. (2009). A new primate from the Eocene Pondaung Formation of Myanmar and the monophyly of Burmese amphipithecids. Proceedings of the Royal Society B: Biological Sciences, 276(1671), 3285-3294.

Beard, K. C., Métais, G., Ocakoğlu, F., and Licht, A. (2020). An omomyid primate from the Pontide microcontinent of north-central Anatolia: Implications for sweepstakes dispersal of terrestrial mammals during the Eocene. Geobios.

Begun, D. R. (1992). Dryopithecus crusafonti sp. nov., a new Miocene hominoid species from Can Ponsic (Northeastern Spain). American Journal of Physical Anthropology, 87(3), 291-309.

Berger, L. R., and Parkington, J. E. (1995). A new Pleistocene hominid-bearing locality at Hoedjiespunt, South Africa. American Journal of Physical Anthropology, 98(4), 601-609.

Bernor, R. L., Flynn, L. J., Harrison, T., Hussain, S. T., and Kelley, J. (1988). Dionysopithecus from southern Pakistan and the biochronology and biogeography of early Eurasian catarrhines. Journal of Human Evolution, 17(3), 339-358.

Bloch, J. I., and Gingerich, P. D. (1998). Carpolestes simpsoni, new species (Mammalia, Proprimates) from the late Paleocene of the Clark's Fork Basin, Wyoming.

Bloch, J. I., Boyer, D. M., Gingerich, P. D., and Gunnell, G. F. (2002). New primitive paromomyid from the Clarkforkian of Wyoming and dental eruption in Plesiadapiformes. Journal of Vertebrate Paleontology, 22(2), 366-379.

Blumenberg, B., and Lloyd, A. T. (1983). Australopithecus and the origin of the genus Homo: Aspects of biometry and systematics with accompanying catalog of tooth metric data. BioSystems, 16(2), 127-167.

Bown, T. M., and Rose, K. D. (1987). Patterns of dental evolution in early Eocene anaptomorphine primates (Omomyidae) from the Bighorn Basin, Wyoming. Memoir (The Paleontological Society), 1-162.

Bown, T. M., and Rose, K. D. (1991). Evolutionary relationships of a new genus and three new species of omomyid primates (Willwood Formation, Lower Eocene, Bighorn Basin, Wyoming). Journal of Human Evolution, 20(6), 465-480.

Boyer, D. M., Costeur, L., and Lipman, Y. (2012). Earliest record of Platychoerops (primates, Plesiadapidae), a new species from Mouras quarry, Mont de Berru, France. American Journal of Physical Anthropology, 149(3), 329-346.

Boyer, D. M., Maiolino, S. A., Holroyd, P. A., Morse, P. E., and Bloch, J. I. (2018). Oldest evidence for grooming claws in euprimates. Journal of Human Evolution, 122, 1-22.

Boyer, D. M., Scott, C. S., and Fox, R. C. (2012). New craniodental material of Pronothodectes gaoi Fox (Mammalia,"Plesiadapiformes") and relationships among members of Plesiadapidae. American Journal of Physical Anthropology, 147(4), 511-550.

Boyer, D. M., Seiffert, E. R., and Simons, E. L. (2010). Astragalar morphology of Afradapis, a large adapiform primate from the earliest late Eocene of Egypt. American Journal of Physical Anthropology, 143(3), 383-402.

Boyer, D. M., Seiffert, E. R., Gladman, J. T., and Bloch, J. I. (2013). Evolution and allometry of calcaneal elongation in living and extinct primates. PloS one, 8(7), e67792.

Brace, C. L. (1979). Krapina,"classic" Neanderthals, and the evolution of the European face. Journal of Human Evolution, 8(5), 527-550.

Brunet, M., Guy, F., Pilbeam, D., Mackaye, H. T., Likius, A., Ahounta, D., ... and Zollikofer, C. (2002). A new hominid from the Upper Miocene of Chad, Central Africa. Nature, 418(6894), 145-151.

Brunet, Michel, Franck Guy, David Pilbeam, Daniel E. Lieberman, Andossa Likius, Hassane T. Mackaye, Marcia S. Ponce de Leon, Christoph P. E. Zollikofer, and Patrick Vignaud. 2005. New material of the earliest hominid from the Upper Miocene of Chad. Nature 434: 752-755.

Buckley, G. A. (1997). A new species of Purgatorius (Mammalia; Primatomorpha) from the lower Paleocene Bear formation, Crazy Mountains basin, south-central Montana. Journal of Paleontology, 149-155.

Burger, B. J. (2010). Skull of the Eocene Primate Omomys carteri from Western North America. Paleontological Contributions, 2010(2), 1-19.

Burger, B. J., and Honey, J. G. (2008). Plesiadapidae (Mammalia, Primates) from the late Paleocene Fort Union Formation of the Piceance Creek Basin, Colorado. Journal of Vertebrate Paleontology, 28(3), 816-825.

Chaimanee, Y. (2004). Siamopithecus eocaenus, anthropoid primate from the late Eocene of Krabi, Thailand. In Anthropoid Origins (pp. 341-368). Springer, Boston, MA.

Chaimanee, Y., Chavasseau, O., Beard, K. C., Kyaw, A. A., Soe, A. N., Sein, C., ... and Jaeger, J. J. (2012). Late Middle Eocene primate from Myanmar and the initial anthropoid colonization of Africa. Proceedings of the National Academy of Sciences, 109(26), 10293-10297.

Chaimanee, Y., Lazzari, V., Benammi, M., Euriat, A., and Jaeger, J. J. (2015). A new small pliopithecoid primate from the Middle Miocene of Thailand. Journal of human evolution, 88, 15-24.

Chaimanee, Y., Lebrun, R., Yamee, C., and Jaeger, J. J. (2011). A new Middle Miocene tarsier from Thailand and the reconstruction of its orbital morphology using a geometric–morphometric method. Proceedings of the Royal Society B: Biological Sciences, 278(1714), 1956-1963.

Chester, S. G., and Bloch, J. I. (2013). Systematics of Paleogene Micromomyidae (Euarchonta, Primates) from North America. Journal of Human Evolution, 65(2), 109-142.

Chornogubsky, L., Diederle, J., Noriega, J., and Fernícola, J. C. NEW PRIMATES FROM THE RÍO SANTA CRUZ AND RÍO BOTE (EARLY–MIDDLE MIOCENE), SANTA CRUZ PROVINCE, ARGENTINA.

Ciochon, R. (Ed.). (2012). New interpretations of ape and human ancestry. Springer Science and Business Media.

Clemens, W. A. (1974). Purgatorius, an early paromomyid primate (Mammalia). Science, 184(4139), 903-905.

Clemens, W. A., Wilson, G. P., and Albright, L. B. (2009). Early Torrejonian mammalian local faunas from northeastern Montana, USA. Museum of Northern Arizona Bulletin, 65, 111-158.

Cooke, S. B., Rosenberger, A. L., and Turvey, S. (2011). An extinct monkey from Haiti and the origins of the Greater Antillean primates. Proceedings of the National Academy of Sciences, 108(7), 2699-2704.

Cote, S., Malit, N., and Nengo, I. (2014). Additional mandibles of Rangwapithecus gordoni, an early Miocene catarrhine from the Tinderet localities of Western Kenya. American journal of physical anthropology, 153(3), 341-352.

Cuozzo (2000) Thesis.

Cuozzo, F. P., Rasoazanabary, E., Godfrey, L. R., Sauther, M. L., Youssouf, I. A., and LaFleur, M. M. (2013). Biological variation in a large sample of mouse lemurs from Amboasary, Madagascar: implications for interpreting variation in primate biology and paleobiology. Journal of human evolution, 64(1), 1-20.

De Bast, E., Gagnaison, C., and Smith, T. (2018). Plesiadapid mammals from the latest Paleocene of France offer new insights on the evolution of Plesiadapis during the Paleocene-Eocene transition. Journal of Vertebrate Paleontology, 38(3), e1460602.

de Bonis, L., and Koufos, G. D. (1993). The face and the mandible of Ouranopithecus macedoniensis: description of new specimens and comparisons. Journal of Human Evolution, 24(6), 469-491.

de Bonis, L., Koufos, G. D., Guy, F., Peigné, S., and Sylvestrou, I. (1998). Nouveaux restes du primate hominoïde Ouranopithecus dans les dépôts du Miocène supérieur de Macédoine (Grèce). Comptes Rendus de l'Académie des Sciences-Series IIA-Earth and Planetary Science, 327(2), 141-146.4

DRAFT

Dutchak, A. R. (2010). Mammalian faunal change during the early Eocene climatic optimum (Wasatchian and Bridgerian) at Raven Ridge in the Northeastern Uinta Basin, Colorado and Utah. University of Colorado at Boulder.

Engelberger, S. (2010). Annotated catalogue of primate type specimens in the mammal collection of the Museum of Natural History Vienna (Doctoral dissertation, uniwien).

Femenias-Gual, J., Marigó, J., Minwer-Barakat, R., and Moyà-Solà, S. (2017). New dental and postcranial material of Agerinia smithorum (Primates, Adapiformes) from the type locality Casa Retjo-1 (early Eocene, Iberian Peninsula). Journal of Human Evolution, 113, 127-136.

Femenias-Gual, J., Minwer-Barakat, R., Marigó, J., and Moyà-Solà, S. (2016). Agerinia smithorum sp. nov., a new early Eocene primate from the Iberian Peninsula. American journal of physical anthropology, 161(1), 116-124.

Fleagle, J. G., and Kay, R. F. (1994). Anthropoid origins. In Anthropoid Origins (pp. 675-698). Springer, Boston, MA.

Fleagle, J. G., and Simons, E. L. (1978). Micropithecus clarki, a small ape from the Miocene of Uganda. American Journal of Physical Anthropology, 49(4), 427-440.

Fleagle, J. G., Powers, D. W., Conroy, G. C., and Watters, J. P. (1987). New fossil platyrrhines from Santa Cruz province, Argentina. Folia primatologica, 48(1-2), 65-77.

Flynn, J. J., Wyss, A. R., Charrier, R., and Swisher, C. C. (1995). An early Miocene anthropoid skull from the Chilean Andes. Nature, 373(6515), 603-607.

Fox, R. C. (1990). Pronothodectes gaoi n. sp. from the late Paleocene of Alberta, Canada, and the early evolution of the Plesiadapidae (Mammalia, Primates). Journal of Paleontology, 637-647.

Fox, R. C. (1991). Saxonella (Plesiadapiformes:? Primates) in North America: S. naylori, sp. nov., from the late Paleocene of Alberta, Canada. Journal of Vertebrate Paleontology, 11(3), 334-349.

Fox, R. C. (2002). The dentition and relationships of Carpodaptes cygneus (Russell)(Carpolestidae, Plesiadapiformes, Mammalia), from the late Paleocene of Alberta, Canada. Journal of Paleontology, 76(5), 864-881.

Franzen, J. L., Gingerich, P. D., Habersetzer, J., Hurum, J. H., Von Koenigswald, W., and Smith, B. H. (2009). Complete primate skeleton from the middle Eocene of Messel in Germany: morphology and paleobiology. PLoS one, 4(5), e5723.

Gabunia, L., and Vekua, A. (1995). A plio-pleistocene hominid from Dmanisi, East Georgia, Caucasus. Nature, 373(6514), 509-512.

Gazin, C. L. (1956). Paleocene mammalian faunas of the Bison Basin in south-central Wyoming. Smithsonian Miscellaneous Collections.

Gazin, C. L. (1958). A review of the middle and upper Eocene primates of North America. Smithsonian Miscellaneous Collections.

Gazin, C. L. (1968). A NEW PRIMATE FROM THETORREJON MIDDLE PALEOCENE OF THE SAN JUAN BASIN, NEW MEXICO. Proc. Biol. Soc. Wash, 81, 629.

Gençturk, I., Alpagut, B., and Andrews, P. (2008). Interproximal wear facets and tooth associations in the Paşalar hominoid sample. Journal of human evolution, 54(4), 480-493.

Gilbert, C. C., Goble, E. D., and Hill, A. (2010). Miocene Cercopithecoidea from the Tugen Hills, Kenya. Journal of Human Evolution, 59(5), 465-483.

Gilbert, C. C., Patel, B. A., Singh, N. P., Campisano, C. J., Fleagle, J. G., Rust, K. L., and Patnaik, R. (2017). New sivaladapid primate from Lower Siwalik deposits surrounding Ramnagar (Jammu and Kashmir State), India. Journal of human evolution, 102, 21-41.

Gingerich, P. D. (1974). Cranial anatomy and evolution of early Tertiary Plesiadapidae (Mammalia, Primates). Yale University.

Gingerich, P. D. (1977). Dental variation in early Eocene Teilhardina belgica, with notes on the anterior dentition of some early Tarsiiformes. Folia Primatologica, 28(2), 144-153.

Gingerich, P. D. (1977). New Species of Eocene Primates and the Phytogeny of European Adapidae. Folia Primatologica, 28(1), 60-80.

Gingerich, P. D. (1978). The Stuttgart collection of Oligocene primates from the Fayum Province of Egypt. Paläontologische Zeitschrift, 52(1), 82-92.

Gingerich, P. D., and Haskin, R. A. (1981). Dentition of early Eocene Pelycodus jarrovii (Mammalia, Primates) and the generic attribution of species formerly referred to Pelycodus.

Gingerich, P. D., Dashzeveg, D., and Russell, D. E. (1991). Dentition and systematic relationships of Altanius orlovi (Mammalia, Primates) from the early Eocene of Mongolia. Geobios, 24(5), 637-646.

Gingerich, P. D., Smith, B. H., and Rosenberg, K. (1982). Allometric scaling in the dentition of primates and prediction of body weight from tooth size in fossils. American Journal of Physical Anthropology, 58(1), 81-100.

Godinot, M. (1998). A summary of adapiform systematics and phylogeny. Folia primatologica, 69(Suppl. 1), 218-249.

Godinot, M., Russell, D. E., and Louis, P. (1992). Oldest known Nannopithex (Primates, Omomyiformes) from the early Eocene of France. Folia Primatologica, 58(1), 32-40.

Gracia-Téllez, A., Arsuaga, J. L., Martínez, I., Martín-Francés, L., Martinón-Torres, M., de Castro, J. M. B., ... and Lira, J. (2013). Orofacial pathology in Homo heidelbergensis: The case of Skull 5 from the Sima de los Huesos site (Atapuerca, Spain). Quaternary International, 295, 83-93.

Gregory, W. K., Hellman, M., and Lewis, G. E. (1938). Fossil anthropoids of the Yale-Cambridge India expedition of 1935 (p. 27). Carnegie institution of Washington.

Gunnell, G. F. (1989). Evolutionary history of Microsyopoidea (Mammalia,? Primates) and the relationship between Plesiadapiformes and Primates.

Gunnell, G. F. (1995). Omomyid primates (Tarsiiformes) from the bridger formation, middle Eocene, southern Green River Basin, Wyoming. Journal of Human Evolution, 28(2), 147-187.

Gunnell, G. F., and Gingerich, P. D. (1981). A new species of Niptomomys (Microsyopidae) from the early Eocene of Wyoming. Folia Primatologica, 36(1-2), 128-137.

Gunnell, G. F., and Miller, E. R. (2001). Origin of Anthropoidea: dental evidence and recognition of early anthropoids in the fossil record, with comments on the Asian anthropoid radiation. American Journal of Physical Anthropology: The Official Publication of the American Association of Physical Anthropologists, 114(3), 177-191.

Haile-Selassie, Y., Gibert, L., Melillo, S. M., Ryan, T. M., Alene, M., Deino, A., ... and Saylor, B. Z. (2015). New species from Ethiopia further expands Middle Pliocene hominin diversity. Nature, 521(7553), 483-488.

Harrison, T. (1981). New finds of small fossil apes from the Miocene locality at Koru in Kenya. Journal of human Evolution, 10(2), 129-137.

Harrison, T. (1986). New fossil anthropoids from the middle Miocene of East Africa and their bearing on the origin of the Oreopithecidae. American Journal of Physical Anthropology, 71(3), 265-284.

Harrison, T. (1988). A taxonomic revision of the small catarrhine primates from the early Miocene of East Africa. Folia Primatologica, 50(1-2), 59-108.

Harrison, T. (1989). A new species of Micropithecus from the middle Miocene of Kenya. Journal of Human Evolution, 18(6), 537-557.

Harrison, T. (1992). A reassessment of the taxonomic and phylogenetic affinities of the fossil catarrhines from Fort Ternan, Kenya. Primates, 33(4), 501-522.

Harrison, T. (2010). Dendropithecoidea, proconsuloidea, and hominoidea. Cenozoic mammals of Africa, 429-469.

Harrison, T., and Yumin, G. (1999). Taxonomy and phylogenetic relationships of early Miocene catarrhines from Sihong, China. Journal of human evolution, 37(2), 225-277.

Harrison, T., Van der Made, J., and Ribot, F. (2002). A new middle Miocene pliopithecid from Sant Quirze, northern Spain. Journal of human evolution, 42(4), 371-377.

Henke, W., and Tattersall, I. (Eds.). (2015). Handbook of paleoanthropology (Vol. 3). Berlin: Springer.

Hill, A., Behrensmeyer, K., Brown, B., Deino, A., Rose, M., Saunders, J., ... and Winkler, A. (1991). Kipsaramon: a lower Miocene hominoid site in the Tugen Hills, Baringo District, Kenya. Journal of Human Evolution, 20(1), 67-75.

Hill, A., Nengo, I. O., and Rossie, J. B. (2013). A Rangwapithecus gordoni mandible from the early Miocene site of Songhor, Kenya. Journal of human evolution, 65(5), 490-500.

Hlusko, L. J. (2007). A new late Miocene species of Paracolobus and other Cercopithecoidea (Mammalia: Primates) fossils from Lemudong'o, Kenya. Kirtlandia, 56(72), e85.

Hlusko, L. J., Carlson, J. P., Guatelli-Steinberg, D., Krueger, K. L., Mersey, B., Ungar, P. S., and Defleur, A. (2013). Neanderthal teeth from moula-guercy, Ardèche, France. American journal of physical anthropology, 151(3), 477-491.

Hooker, J. J. (2007). A new microchoerine omomyid (Primates, Mammalia) from the English early Eocene and its palaeobiogeographical implications. Palaeontology, 50(3), 739-756.

Hooker, J. J., and Harrison, D. L. (2008). A new clade of omomyid primates from the European Paleogene. Journal of Vertebrate Paleontology, 28(3), 826-840.

Hooker, J. J., Russell, D. E., and Phélizon, A. (1999). A new family of Plesiadapiformes (Mammalia) from the Old World lower Paleogene. Palaeontology, 42(3), 377-407.

Horovitz, I., and MacPhee, R. D. (1999). The quaternary Cuban platyrrhineParalouatta varonaiand the origin of Antillean monkeys. Journal of Human Evolution, 36(1), 33-68.

Hublin, Jean-Jacques and Ben-Ncer, Abdelouahed and Bailey, Shara E. and Freidline, Sarah E. and Neubauer, Simon and Skinner, Matthew M. and Bergmann, Inga and Le Cabec, Adeline and Benazzi, Stefano and Harvati, Katerina and Gunz, Philipp (2017) New fossils from Jebel Irhoud, Morocco and the pan-African origin of Homo sapiens. Nature, 546 (7657). pp. 289-292. ISSN

Imbrasas, M. D. (2018). Performance of 2D geometric morphometric analysis in hominin taxonomy and its application to the mandibular molar sample from Lomekwi, Kenya (Doctoral dissertation, University of Kent,).

Jacobs, L. L. (1981). Miocene lorisid primates from the Pakistan Siwaliks. Nature, 289(5798), 585-587.

Jaeger, J. J., Beard, K. C., Chaimanee, Y., Salem, M., Benammi, M., Hlal, O., ... and Brunet, M. (2010). Late middle Eocene epoch of Libya yields earliest known radiation of African anthropoids. Nature, 467(7319), 1095-1098.

Jaeger, J. J., Chavasseau, O., Lazzari, V., Soe, A. N., Sein, C., Le Maître, A., ... and Chaimanee, Y. (2019). New Eocene primate from Myanmar shares dental characters with African Eocene crown anthropoids. Nature communications, 10(1), 1-10.

Jaeger, J. J., Thein, T., Benammi, M., Chaimanee, Y., Soe, A. N., Lwin, T., ... and Ducrocq, S. (1999). A new primate from the middle Eocene of Myanmar and the Asian early origin of anthropoids. Science, 286(5439), 528-530.

Kay, R. F. (1982). Sivapithecus simonsi, a new species of Miocene hominoid, with comments on the phylogenetic status of the Ramapithecinae. International Journal of Primatology, 3(2), 113-173.

Kay, R. F. (1993). Large fossil platyrrhines from the Rio Acre local fauna, late Miocene, western Amazonia. J. Hum. Evol., 25, 319-327.

Kay, R. F. (1994). "Giant" tamarin from the Miocene of Colombia. American Journal of Physical Anthropology, 95(3), 333-353.

Kay, R. F. (1997). A new small platyrrhine and the phyletic position of callitrichinae. Vertebrate Paleontology in the Neotropics: the Miocene fauna of La Venta, Colombia, 435-458.

DRAFT

Kay, R. F. (2010). A new primate from the early Miocene of Gran Barranca, Chubut Province, Argentina: Paleoecological implications. The Paleontology of Gran Barranca: Evolution and Environmental Change through the Middle Cenozoic of Patagonia. Cambridge University Press, Cambridge, 220-239.

Kay, R. F., and Cozzuol, M. A. (2006). New platyrrhine monkeys from the Solimões formation (late Miocene, Acre State, Brazil). Journal of Human Evolution, 50(6), 673-686.

Kay, R. F., and Simons, E. L. (1980). The ecology of oligocene African anthropoidea. International Journal of Primatology, 1(1), 21-37.

Kay, R. F., and Ungar, P. S. (1997). Dental evidence for diet in some Miocene catarrhines with comments on the effects of phylogeny on the interpretation of adaptation. In Function, phylogeny, and fossils (pp. 131-151). Springer, Boston, MA

Kay, R. F., and Ungar, P. S. (1997). Dental evidence for diet in some Miocene catarrhines with comments on the effects of phylogeny on the interpretation of adaptation. In Function, phylogeny, and fossils (pp. 131-151). Springer, Boston, MA.

Kay, R. F., Fleagle, J. G., and Simons, E. L. (1981). A revision of the Oligocene apes of the Fayum Province, Egypt. American Journal of Physical Anthropology, 55(3), 293-322.

Kay, R. F., Fleagle, J. G., Mitchell, T. R. T., Colbert, M., Bown, T., and Powers, D. W. (2008). The anatomy of Dolichocebus gaimanensis, a stem platyrrhine monkey from Argentina. Journal of Human Evolution, 54(3), 323-382.

Kay, R. F., Gonzales, L. A., Salenbien, W., Martinez, J. N., Cooke, S. B., Valdivia, L. A., ... and Baker, P. A. (2019). Parvimico materdei gen. et sp. nov.: A new platyrrhine from the Early Miocene of the Amazon Basin, Peru. Journal of human evolution, 134, 102628.

Kay, R. F., Madden, R. H., Plavcan, J. M., Cifelli, R. L., and Díaz, J. G. (1987). Stirtonia victoriae, a new species of Miocene Colombian primate. Journal of Human Evolution, 16(2), 173-196.

Kay, R. F., Perry, J. M., Malinzak, M. D., Allen, K. L., Kirk, E. C., Plavcan, J. M., and Fleagle, J. G. (2012). The paleobiology of Santacrucian primates. Early Miocene Paleobiology in Patagonia: High-Latitude Paleocommunities of the Santa Cruz Formation, 306-330.

Kay, R., Madden, R. H., and Guerrero-Diaz, J. (1989). Nuevos hallazgos de monos en el Mioceno de Colombia. Ameghiniana, 25(3), 203-212.

Kelley, J. (1988). A new large species of Sivapithecus from the Siwaliks of Pakistan. Journal of Human Evolution, 17(3), 305-324.

Kelley, J., Ward, S., Brown, B., Hill, A., Duren, D.L., 2002. Dental remains of Equatorius africanus from Kipsaramon, Tugen Hills, Baringo District, Kenya. J. Hum. Evol. 42, 39-62.

Kelly, T. S., and Murphey, P. C. (2016). Mammals from the earliest Uintan (middle Eocene) Turtle Bluff Member, Bridger Formation, southwestern Wyoming, USA, Part 1: Primates and Rodentia. Palaeontol. Electron, 19, 1-55.

Kirk, E. C., and Simons, E. L. (2001). Diets of fossil primates from the Fayum Depression of Egypt: a quantitative analysis of molar shearing. Journal of Human Evolution, 40(3), 203-229.

Kirk, E. C., and Williams, B. A. (2011). New adapiform primate of Old World affinities from the Devil's Graveyard Formation of Texas. Journal of Human Evolution, 61(2), 156-168.

Kordos, L., and Begun, D. R. (1997). A new reconstruction of RUD 77, a partial cranium of Dryopithecus brancoi from Rudabánya, Hungary. American Journal of Physical Anthropology: The Official Publication of the American Association of Physical Anthropologists, 103(2), 277-294.

Koufos, G. D. (1993). Mandible of Ouranopithecus macedoniensis (Hominidae, Primates) from a new late Miocene locality of Macedonia (Greece). American Journal of Physical Anthropology, 91(2), 225-234.

Koufos, G. D. (1995). The first female maxilla of the hominoid Ouranopithecus macedoniensis from the late Miocene of Macedonia, Greece. Journal of Human Evolution, 29(4), 385-399.

Krause, D. W., and Gingerich, P. D. (1983). Mammalian fauna from Douglass Quarry, earliest Tiffanian (late Paleocene) of the eastern Crazy Mountain Basin, Montana.

KUNIMATSU, Y. (1992). A revision of the hypodigm of Nyanzapithecus vancouveringi. African Study Monographs, 13(4), 231-235.

Kunimatsu, Y., Ratanasthien, B., Nakaya, H., Saegusa, H., and Nagaoka, S. (2004). Earliest Miocene hominoid from Southeast Asia. American Journal of Physical Anthropology: The Official Publication of the American Association of Physical Anthropologists, 124(2), 99-108.

Kunimatsu, Y., Ratanasthien, B., Nakaya, H., Saegusa, H., Nagaoka, S., Suganuma, Y., ... and Udomkan, B. (2005). An additional specimen of a large-bodied Miocene hominoid from Chiang Muan, northern Thailand. Primates, 46(1), 65-70.

Lannoye, E. K. (2015). A New Middle Paleocene Mammalian Fauna from the Fort Union Formation, Great Divide Basin, Wyoming.

Leakey, L. S. B. (1968). Lower dentition of Kenyapithecus africanus. Nature, 217(5131), 827-830.

Leakey, M. G., Spoor, F., Brown, F. H., Gathogo, P. N., Kiarie, C., Leakey, L. N., and McDougall, I. (2016). New hominin genus from eastern Africa shows diverse middle Pliocene lineages. In Human Evolution Source Book (pp. 118-127). Routledge.

Leakey, M. G., Ungar, P. S., and Walker, A. (1995). A new genus of large primate from the late Oligocene of Lothidok, Turkana District, Kenya. Journal of Human Evolution, 28(6), 519-531.

Leakey, R. E., Leakey, M. G., and Walker, A. C. (1988). Morphology of Afropithecus turkanensis from Kenya. American Journal of Physical Anthropology, 76(3), 289-307.

Leakey, R. E., Leakey, M. G., and Walker, A. C. (1988). Morphology of Turkanapithecus kalakolensis from Kenya. American Journal of Physical Anthropology, 76(3), 277-288.

Lillegraven, J. A. (1980). Primates from later Eocene rocks of southern California. Journal of Mammalogy, 61(2), 181-204.

Liu, W., and Zheng, L. (2005). Comparisons of tooth size and morphology between the late Miocene hominoids from Lufeng and Yuanmou, China, and their implications. Anthropological Science, 113(1), 73-77.

López-Torres, S. (2017). The Paromomyidae (Primates, Mammalia): Systematics, Evolution, and Ecology (Doctoral dissertation, University of Toronto (Canada)).

López-Torres, S., and Silcox, M. T. (2018). The European Paromomyidae (Primates, Mammalia): taxonomy, phylogeny, and biogeographic implications. Journal of Paleontology, 92(5), 920-937.

López-Torres, S., Silcox, M. T., and Holroyd, P. A. (2018). New omomyoids (Euprimates, Mammalia) from the late Uintan of southern California, USA, and the question of the extinction of the Paromomyidae (Plesiadapiformes, Primates). PALAEONTOLOGIA ELECTRONICA, 21(3).

MacDonald, T. E. (1996). Late Paleocene (Tiffanian) mammal-bearing localities in superposition, from near Drumheller, Alberta.

MacInnes, D. G. (1943). Notes on the east African Miocene primates. Journal of the East Africa and Uganda Natural History Society, 17(3-4), 141-181.

MacPhee, R. D., and Horovitz, I. (2004). New Craniodental Remains of the Quaternary Jamaican Monkey Xenothrix mcgregori (Xenotrichini, Callicebinae, Pitheciidae), with a Reconsideration of the Aotus Hypothesis1. American Museum Novitates, 2004(3434), 1-51.

Madden, C. T., and Lewis, G. E. (1980). Indopithecus giganteus distinct fromSivapithecus indicus. Primates, 21(4), 572-576.

Malassé, A. D., Zhang, P., and Wils, P. (2018). A new molar from the Middle Pleistocene hominid assemblage of Yanhuidong, Tongzi, South China. Acta Anthropologica Sinica, 37, 1-17.

Marigó, J., Minwer-Barakat, R., and Moyà-Solà, S. (2013). Nievesia sossisensis, a new anchomomyin (Adapiformes, Primates) from the early Late Eocene of the southern Pyrenees (Catalonia, Spain). Journal of Human Evolution, 64(6), 473-485.

Marigó, J., Susanna, I., Minwer-Barakat, R., Madurell-Malapeira, J., Moyà-Solà, S., Casanovas-Vilar, I., ... and Alba, D. M. (2014). The primate fossil record in the Iberian Peninsula. Journal of Iberian Geology, 40(1), 179-211.

Marivaux, L., Adnet, S., Altamirano-Sierra, A. J., Boivin, M., Pujos, F., Ramdarshan, A., ... and Antoine, P. O. (2016). Neotropics provide insights into the emergence of New World monkeys: New dental evidence from the late Oligocene of Peruvian Amazonia. Journal of Human Evolution, 97, 159-175.

Marivaux, L., Aguirre-Diaz, W., Benites-Palomino, A., Billet, G., Boivin, M., Pujos, F., ... and Antoine, P. O. (2020). New record of Neosaimiri (Cebidae, Platyrrhini) from the late Middle Miocene of Peruvian Amazonia. Journal of Human Evolution, 146, 102835.

Marivaux, L., Antoine, P. O., Baqri, S. R. H., Benammi, M., Chaimanee, Y., Crochet, J. Y., ... and Welcomme, J. L. (2005). Anthropoid primates from the Oligocene of Pakistan (Bugti Hills): data on early anthropoid evolution and biogeography. Proceedings of the National Academy of Sciences, 102(24), 8436-8441.

Maschenko, E. N., and Takai, M. (2010). Primates of the genus Altanius (Mammalia, Primates) from the Lower Eocene of Tsagan-Khushu, southern Mongolia. Russ. J. Theriol, 9(2), 61-69.

Mason, M. A. (1990). New fossil primates from the Uintan (Eocene) of southern California. Museum of Paleontology, University of California.

Matsumura, H., Cuong, N. L., Thuy, N. K., and Anezaki, T. (2001). Dental morphology of the early Hoabinian, the Neolithic Da But and the Metal Age Dong Son civilized peoples in Vietnam. Zeitschrift für Morphologie und anthropologie, 59-73.

Mattingly, S. G., Beard, K. C., Coster, P. M., Salem, M. J., Chaimanee, Y., and Jaeger, J. J. (2021). A new parapithecine (Primates: Anthropoidea) from the early Oligocene of Libya supports parallel evolution of large body size among parapithecids. Journal of Human Evolution, 153, 102957.

McCrossin, M. L. (1992). New species of bushbaby from the middle Miocene of Maboko Island, Kenya. American Journal of Physical Anthropology, 89(2), 215-233.

McNulty, K. P., Begun, D. R., Kelley, J., Manthi, F. K., and Mbua, E. N. (2015). A systematic revision of Proconsul with the description of a new genus of early Miocene hominoid. Journal of Human Evolution, 84, 42-61.

Meldrum, D. J., and Kay, R. F. (1997). Nuciruptor rubricae, a new pitheciin seed predator from the Miocene of Colombia. American Journal of Physical Anthropology: The Official Publication of the American Association of Physical Anthropologists, 102(3), 407-427.

Menz, U. M. (2016). Evolution und Funktionsvariabilität von bunodonten Molaren bei Primaten (Doctoral dissertation, Johann Wolfgang Goethe-Universität in Frankfurt am Main).

Miller, E. R., Benefit, B. R., McCrossin, M. L., Plavcan, J. M., Leakey, M. G., El-Barkooky, A. N., ... and Simons, E. L. (2009). Systematics of early and middle Miocene Old World monkeys. Journal of Human Evolution, 57(3), 195-211.

Minwer-Barakat, R., Marigó, J., Becker, D., and Costeur, L. (2017). A new primate assemblage from La Verrerie de Roches (Middle Eocene, Switzerland). Journal of human evolution, 113, 137-154.

Minwer-Barakat, R., Marigó, J., Femenias-Gual, J., and Moyà-Solà, S. (2015). New material of Pseudoloris parvulus (Microchoerinae, Omomyidae, Primates) from the late Eocene of Sossís (Northeastern Spain) and its implications for the evolution of Pseudoloris. Journal of Human Evolution, 83, 74-90.

Morris, W. J. (1954). An Eocene fauna from the Cathedral Bluffs Tongue of the Washakie Basin, Wyoming. Journal of Paleontology, 195-203.

Morse, P. E., Chester, S. G., Boyer, D. M., Smith, T., Smith, R., Gigase, P., and Bloch, J. I. (2019). New fossils, systematics, and biogeography of the oldest known crown primate Teilhardina from the earliest Eocene of Asia, Europe, and North America. Journal of human evolution, 128, 103-131.

Moyà-Solà, S., Köhler, M., Alba, D. M., Casanovas-Vilar, I., Galindo, J., Robles, J. M., ... and Beamud, E. (2009). First partial face and upper dentition of the Middle Miocene hominoid Dryopithecus fontani from Abocador

DRAFT

de Can Mata (Vallès-Penedès Basin, Catalonia, NE Spain): Taxonomic and phylogenetic implications. American Journal of Physical Anthropology: The Official Publication of the American Association of Physical Anthropologists, 139(2), 126-145.

Muldoon, K. M., and Gunnell, G. F. (2002). Omomyid primates (Tarsiiformes) from the Early Middle Eocene at South Pass, Greater Green River Basin, Wyoming. Journal of human evolution, 43(4), 479-511.

Murphey, P. C., and Dunn, R. H. (2009). Hemiacodon engardae, a new species of omomyid primate from the earliest Uintan Turtle Bluff Member of the Bridger Formation, southwestern Wyoming, USA. Journal of human evolution, 57(2), 123-130.

Nelson, M. E. (1977). Middle Eocene primates (Mammalia) from southwestern Wyoming. The Southwestern Naturalist, 487-493.

Nengo, I. O., and Rae, T. C. (1992). New hominoid fossils from the early Miocene site of Songhor, Kenya. Journal of Human Evolution, 23(5), 423-429.

Neumann, A. M. (2013). A new Early Eocene (Lostcabinian) mammal assemblage from the Main Body of the Wasatch Formation, Northern Green River Basin; The Pinnacles, Sweetwater Co., Wyoming.

NEW SPECIMENS OF ELPHIDOTARSIUS RUSSELLI (MAMMALIA, ?PRIMATES, CARPOLESTIDAE) AND A REVISION OF PLESIADAPOID RELATIONSHIPS

Ni, X., Hu, Y., Wang, Y., and LI, C. (2004). A clue to the Asian origin of euprimates. Anthropological Science, 0408100017-0408100017.

Ni, X., Li, Q., Li, L., and Beard, K. C. (2016). Oligocene primates from China reveal divergence between African and Asian primate evolution. Science, 352(6286), 673-677.

Ni, X., Meng, J., Beard, K. C., Gebo, D. L., Wang, Y., and Li, C. (2010). A new tarkadectine primate from the Eocene of Inner Mongolia, China: phylogenetic and biogeographic implications. Proceedings of the Royal Society B: Biological Sciences, 277(1679), 247-256.

Novo, N. M., and Fleagle, J. G. (2015). New Specimens of Platyrrhine Primates from Patagonia (Pinturas Formation, Early Miocene). Ameghiniana, 52(3), 367-372.

Novo, N. M., Tejedor, M. F., Pérez, M. E., and Krause, J. M. (2017). New primate locality from the early Miocene of Patagonia, Argentina. American journal of physical anthropology, 164(4), 861-867.

Patel, Biren A., and Ari Grossman. "Dental metric comparisons of Morotopithecus and Afropithecus: Implications for the validity of the genus Morotopithecus." Journal of human evolution 51.5 (2006): 506-512.

Patnaik, R., Cameron, D., Sharma, J. C., and HOGARTH, J. (2004). Extinction of Siwalik fossil apes: a review based on a new fossil tooth and on palaeoecological and palaeoclimatological evidence. Anthropological Science, 0408100020-0408100020.

Perry, J. M., Kay, R. F., Vizcaíno, S. F., and Bargo, M. S. (2014). Oldest known cranium of a juvenile New World monkey (Early Miocene, Patagonia, Argentina): implications for the taxonomy and the molar eruption pattern of early platyrrhines. Journal of Human Evolution, 74, 67-81.

Pickford, M. (1985). A new look at Kenyapithecus based on recent discoveries in western Kenya. Journal of Human Evolution, 14(2), 113-143.

Pickford, M., and Kunimatsu, Y. (2005). Catarrhines from the Middle Miocene (ca. 14.5 Ma) of Kipsaraman, Tugen Hills, Kenya. Anthropological Science, 113(2), 189-224.

Pickford, M., Senut, B., Gommery, D., and Musiime, E. (2009). La distinción entre Ugandapithecus y Proconsul. Estudios geológicos, 65(2), 183-241.

Pilbeam, D. (1982). New hominoid skull material from the Miocene of Pakistan. Nature, 295(5846), 232-234.

Pilbeam, D. R., and Pilbeam, D. R. (1969). Tertiary Pongidae of East Africa: evolutionary relationships and taxonomy (pp. 1-185). Peabody Museum of Natural History.

Rasmussen, D. T., Shekelle, M., Walsh, S. L., and Riney, B. O. (1995). The dentition of Dyseolemur, and comments on the use of the anterior teeth in primate systematics. Journal of human evolution, 29(4), 301-320.

Robinson, P. (1966). Fossil Mammalia of the Huerfano Formation, Eocene, of Colorado (Vol. 21). Peabody Museum of Natural History, Yale University.

Robinson, P. (2018). Diversity starts early: notharctid primates from the Sandcouleean (Early Eocene) of the Powder River Basin, Wyoming, USA. Historical Biology, 30(1-2), 189-203.

Rose, K. D. (1975). The Carpolestidae, early tertiary primates from North America. Museum of Comparative Zoology, Harvard University.

Rose, K. D. (1995). Anterior dentition and relationships of the early Eocene omomyids Arapahovius advena and Teilhardina demissa, sp. nov. Journal of Human Evolution, 28(3), 231-244.

Rose, K. D., and Bown, T. M. (1991). Additional fossil evidence on the differentiation of the earliest euprimates. Proceedings of the National Academy of Sciences, 88(1), 98-101.

Rose, K. D., Chester, S. G., Dunn, R. H., Boyer, D. M., and Bloch, J. I. (2011). New fossils of the oldest North American euprimate Teilhardina brandti (Omomyidae) from the Paleocene–Eocene thermal maximum. American journal of physical anthropology, 146(2), 281-305.

Rose, K. D., Chester, S. G., Dunn, R. H., Boyer, D. M., and Bloch, J. I. (2011). New fossils of the oldest North American euprimate Teilhardina brandti (Omomyidae) from the Paleocene–Eocene thermal maximum. American journal of physical anthropology, 146(2), 281-305.'

Rose, K. D., Chester, S. G., Dunn, R. H., Boyer, D. M., and Bloch, J. I. (2011). New fossils of the oldest North American euprimate Teilhardina brandti (Omomyidae) from the Paleocene–Eocene thermal maximum. American journal of physical anthropology, 146(2), 281-305.

Rose, K. D., Chew, A. E., Dunn, R. H., Kraus, M. J., Fricke, H. C., and Zack, S. P. (2012). Earliest Eocene mammalian fauna from the Paleocene-Eocene thermal maximum at sand creek divide, southern Bighorn Basin, Wyoming.

Rose, K. D., MacPhee, R. D., and Alexander, J. P. (1999). Skull of early Eocene Cantius abditus (Primates: Adapiformes) and its phylogenetic implications, with a reevaluation of "Hesperolemur" actius. American Journal of Physical Anthropology: The Official Publication of the American Association of Physical Anthropologists, 109(4), 523-539.

Rosenberger, A. L. (2011). The face of Strigorhysis: implications of another tarsier-like, large-eyed Eocene North American tarsiiform primate. The Anatomical Record: Advances in Integrative Anatomy and Evolutionary Biology, 294(5), 797-812.

Rosenberger, A. L., Klukkert, Z. S., Cooke, S. B., and Rímoli, R. (2013). Rethinking Antillothrix: the mandible and its implications. American Journal of Primatology, 75(8), 825-836.

Rossie, J. B., and Hill, A. (2018). A new species of Simiolus from the middle Miocene of the Tugen Hills, Kenya. Journal of human evolution, 125, 50-58.

Rossie, J. B., and MacLatchy, L. (2006). A new pliopithecoid genus from the early Miocene of Uganda. Journal of human evolution, 50(5), 568-586.

Ruiz-Ramoni, D., Rincón, A. D., Solórzano, A., and Moyà-Solà, S. (2017). The first fossil Platyrrhini (Primates: anthropoidea) from Venezuela: a capuchin monkey from the Plio-Pleistocene of El Breal de Orocual. Journal of human evolution, 105, 127-131.

Rust, K. (2018). An Investigation of the Phylogenetic Affinities of Sivaladapidae within Adapoidea.

Samuels, J. X., Albright, L. B., and Fremd, T. J. (2015). The last fossil primate in N orth A merica, new material of the enigmatic E kgmowechashala from the A rikareean of O regon. American Journal of Physical Anthropology, 158(1), 43-54.

Sankhyan, A. R., Kelley, J., and Harrison, T. (2017). A highly derived pliopithecoid from the Late Miocene of Haritalyangar, India. Journal of human evolution, 105, 1-12.

Secord, R. (2008). The Tiffanian land-mammal age (middle and late Paleocene) in the northern Bighorn Basin, Wyoming.

Seiffert, E. R. (2012). Early primate evolution in Afro-Arabia. Evolutionary Anthropology: Issues, News, and Reviews, 21(6), 239-253.

Seiffert, E. R., Perry, J. M., Simons, E. L., and Boyer, D. M. (2009). Convergent evolution of anthropoid-like adaptations in Eocene adapiform primates. Nature, 461(7267), 1118-1121.

Seiffert, E. R., Simons, E. L., and Attia, Y. (2003). Fossil evidence for an ancient divergence of lorises and galagos. Nature, 422(6930), 421-424.

Seiffert, E. R., Simons, E. L., Boyer, D. M., Perry, J. M., Ryan, T. M., and Sallam, H. M. (2010). A fossil primate of uncertain affinities from the earliest late Eocene of Egypt. Proceedings of the National Academy of Sciences, 107(21), 9712-9717.

Seiffert, E. R., Simons, E. L., Clyde, W. C., Rossie, J. B., Attia, Y., Bown, T. M., ... and Mathison, M. E. (2005). Basal anthropoids from Egypt and the antiquity of Africa's higher primate radiation. Science, 310(5746), 300-304.

Seiffert, E. R., Simons, E. L., Fleagle, J. G., and Godinot, M. (2010). Paleogene Anthropoids. In L. Werdelin (Ed.), Cenozoic Mammals of Africa (pp. 369–392). University of California Press. https://doi.org/10.1525/california/9780520257214.003

Seiffert, E. R., Simons, E. L., Ryan, T. M., and Attia, Y. (2005). Additional remains of Wadilemur elegans, a primitive stem galagid from the late Eocene of Egypt. Proceedings of the National Academy of Sciences, 102(32), 11396-11401.

Seiffert, E. R., Tejedor, M. F., Fleagle, J. G., Novo, N. M., Cornejo, F. M., Bond, M., ... and Campbell, K. E. (2020). A parapithecid stem anthropoid of African origin in the Paleogene of South America. Science, 368(6487), 194-197.

Setoguchi, T., and Rosenberger, A. L. (1987). A fossil owl monkey from La Venta, Colombia. Nature, 326(6114), 692-694.

Setoguchi, T., Shigehara, N., Rosenberger, A. L., and Cadena G, A. (1986). Primate fauna from the Miocene La Venta, in the Tatacoa desert, department of Huila, Colombia. Caldasia, 761-773.

Silcox, M. T., Gunnell, G. F., and Bloch, J. I. (2020). Cranial anatomy of Microsyops annectens (Microsyopidae, Euarchonta, Mammalia) from the middle Eocene of Northwestern Wyoming. Journal of Paleontology, 94(5), 979-1006.

Simons, E. (1995). Egyptian Oligocene primates: a review. American Journal of Physical Anthropology, 38(S21), 199-238.

Simons, E. L. (1961). The dentition of Ourayia: its bearing on relationships of omomyid prosimians. Postilla, 54, 1-20.

Simons, E. L. (1969). Miocene monkey (Prohylobates) from northern Egypt. Nature, 223(5207), 687-689.

Simons, E. L. (1989). Description of two genera and species of Late Eocene Anthropoidea from Egypt. Proceedings of the National Academy of Sciences, 86(24), 9956-9960.

Simons, E. L. (1992). Diversity in the early Tertiary anthropoidean radiation in Africa. Proceedings of the National Academy of Sciences, 89(22), 10743-10747.

Simons, E. L. (1995). Crania of Apidium: primitive anthropoidean (Primates, Parapithecidae) from the Egyptian Oligocene. American Museum novitates; no. 3124.

Simons, E. L. (1997). Preliminary description of the cranium of Proteopithecus sylviae, an Egyptian late Eocene anthropoidean primate. Proceedings of the National Academy of Sciences, 94(26), 14970-14975.

Simons, E. L., and Bown, T. M. (1985). Afrotarsius chatrathi, first tarsiiform primate (? Tarsiidae) from Africa. Nature, 313(6002), 475-477.

Simons, E. L., and EL, S. (1974). PARAPITHECUS GRANGERI (PARAPITHECIDAE, OLD WORLD HIGHER PRIMATES) NEW SPECIES FROM THE OLIGOCENE OF EGYPT AND THE INITIAL DIFFERENTIATION OF CERCOPITHECOIDEA.

Simons, E. L., and Kay, R. F. (1983). Qatrania, new basal anthropoid primate from the Fayum, Oligocene of Egypt. Nature, 304(5927), 624-626.

Simons, E. L., and Kay, R. F. (1988). New material of Qatrania from Egypt with comments on the phylogenetic position of the Parapithecidae (Primates, Anthropoidea). American journal of primatology, 15(4), 337-347.

Simons, E. L., and Rasmussen, D. T. (1991). The generic classification of Fayum Anthropoidea. International journal of primatology, 12(2), 163-178.

DRAFT

Simons, E. L., and Rasmussen, D. T. (1994). A remarkable cranium of Plesiopithecus teras (Primates, Prosimii) from the Eocene of Egypt. Proceedings of the National Academy of Sciences, 91(21), 9946-9950.

Simons, E. L., Rasmussen, D. T., and Gebo, D. L. (1987). A new species of Propliopithecus from the Fayum, Egypt. American journal of physical anthropology, 73(2), 139-147.

Simons, E. L., Seiffert, E. R., Chatrath, P. S., and Attia, Y. (2001). Earliest record of a parapithecid anthropoid from the Jebel Qatrani Formation, northern Egypt. Folia Primatologica, 72(6), 316-331.

Simons, E. L., Seiffert, E. R., Ryan, T. M., and Attia, Y. (2007). A remarkable female cranium of the early Oligocene anthropoid Aegyptopithecus zeuxis (Catarrhini, Propliopithecidae). Proceedings of the National Academy of Sciences, 104(21), 8731-8736.

Simons, Elwyn. "Egyptian Oligocene primates: a review." American Journal of Physical Anthropology 38.S21 (1995): 199-238.

Simpson, G. G. (1937). The Fort Union of the Crazy Mountain field, Montana, and its mammalian faunas. Bulletin of the United States National Museum.

Simpson, G. G., and Granger, W. (1935). The Tiffany fauna, Upper Paleocene. 3, Primates, Carnivora, Condylarthra, and Amblypoda. American Museum novitates; no. 817.

Skinner, M. M., Leakey, M. G., Leakey, L. N., Manthi, F. K., and Spoor, F. (2020). Hominin dental remains from the Pliocene localities at Lomekwi, Kenya (1982–2009). Journal of Human Evolution, 145, 102820.

Smith, T., Rose, K. D., and Gingerich, P. D. (2006). Rapid Asia–Europe–North America geographic dispersal of earliest Eocene primate Teilhardina during the Paleocene–Eocene thermal maximum. Proceedings of the National Academy of Sciences, 103(30), 11223-11227.

Solà, S. M., and Köhler, M. (1995). New partial cranium of Dryopithecus Lartet, 1863 (Hominoidea, Primates) from the upper Miocene of Can Llobateres, Barcelona, Spain. Journal of Human Evolution, 29(2), 101-139.

Stevens, N. J., Seiffert, E. R., O'Connor, P. M., Roberts, E. M., Schmitz, M. D., Krause, C., ... and Temu, J. (2013). Palaeontological evidence for an Oligocene divergence between Old World monkeys and apes. Nature, 497(7451), 611-614.

Stock, C. (1934). Microsyopsinae and Hyopsodontidae in the Sespe Upper Eocene, California. Proceedings of the National Academy of Sciences of the United States of America, 20(6), 349.

Stock, C. (1938). A tarsiid primate and a mixodectid from the Poway Eocene, California. Proceedings of the National Academy of Sciences of the United States of America, 24(7), 288.

Suwa, G. E. N., Asfaw, B., Haile-Selassie, Y., White, T. I. M., Katoh, S., WoldeGabriel, G., ... and Beyene, Y. (2007). Early pleistocene Homo erectus fossils from konso, southern Ethiopia. Anthropological Science, 0705240005-0705240005.

Szalay, F. S. (1976). Systematics of the Omomyidae (Tarsiiformes, Primates): taxonomy, phylogeny, and adaptations. Bulletin of the AMNH; v. 156, article 3.

Takai, M. (1994). New specimens of Neosaimiri fieldsi from La Venta, Colombia: a middle Miocene ancestor of the living squirrel monkeys. Journal of Human Evolution, 27(4), 329-360.

Takai, M., and Anaya, F. (1996). New specimens of the oldest fossil platyrrhine, Branisella boliviana, from Salla, Bolivia. American Journal of Physical Anthropology: The Official Publication of the American Association of Physical Anthropologists, 99(2), 301-317.

Takai, M., Anaya, F., Shigehara, N., and Setoguchi, T. (2000). New fossil materials of the earliest New World monkey, Branisella boliviana, and the problem of platyrrhine origins. American Journal of Physical Anthropology: The Official Publication of the American Association of Physical Anthropologists, 111(2), 263-281.

Takai, M., Anaya, F., Suzuki, H., Shigehara, N., and Setoguchi, T. (2001). A new platyrrhine from the Middle Miocene of La Venta, Colombia, and the phyletic position of Callicebinae. Anthropological Science, 109(4), 289-307.

Takai, M., Nishimura, T., Shigehara, N., and Setoguch, T. (2009). Meaning of the canine sexual dimorphism in fossil owl monkey, Aotus dindensis from the middle Miocene of La Venta, Colombia. In Comparative Dental Morphology (Vol. 13, pp. 55-59). Karger Publishers.

TejedOr, M. F., and Rosenberger, A. L. (2008). A neotype for Homunculus patagonicus Ameghino, 1891, and a new interpretation of the taxon. PaleoAnthropology, 2008, 68-82.

Tornow, M. A. (2008). Systematic analysis of the Eocene primate family Omomyidae using gnathic and postcranial data. Bulletin of the Peabody Museum of Natural History, 49(1), 43-129.

Trinkaus, E. (1978). Dental remains from the Shanidar adult Neanderthals. Journal of Human evolution, 7(5), 369-382.

Van den Bergh, G. D., Kaifu, Y., Kurniawan, I., Kono, R. T., Brumm, A., Setiyabudi, E., ... and Morwood, M. J. (2016). Homo floresiensis-like fossils from the early Middle Pleistocene of Flores. Nature, 534(7606), 245-248.

Wang, W. (2009). New discoveries of Gigantopithecus blacki teeth from Chuifeng Cave in the Bubing Basin, Guangxi, south China. Journal of Human Evolution, 57(3), 229-240.

Wang, X., and Barnes, L. G. (Eds.). (2008). Paleocene primates from the Goler Formation of the Mojave Desert in California (No. 41). Natural History Museum of Los Angeles County.

Webb, M. W. (1996). Late Paleocene mammals from near Drayton Valley, Alberta.

West, R. M. (1982). Fossil mammals from the lower Buck Hill Group, Eocene of Trans-Pecos Texas: Marsupicarnivora, Primates, Taeniodonta, Condylarthra, bunodont Artiodactyla, and Dinocerata. Texas Memorial Museum, The University of Texas at Austin.

Westgate, J. W. (1990). Uintan land mammals (excluding rodents) from an estuarine facies of the Laredo Formation (middle Eocene, Claiborne Group) of Webb County, Texas. Journal of Paleontology, 454-468.

Wheeler, B. C. (2010). Community ecology of the Middle Miocene primates of La Venta, Colombia: the relationship between ecological diversity, divergence time, and phylogenetic richness. Primates, 51(2), 131-138.

White, T. D., Suwa, G., and Asfaw, B. (1994). Australopithecus ramidus, a new species of early hominid from Aramis, Ethiopia. Nature, 371(6495), 306-312.

White, T. D., Suwa, G., Simpson, S., and Asfaw, B. (2000). Jaws and teeth of Australopithecus afarensis from Maka, Middle Awash, Ethiopia. American Journal of Physical Anthropology: The Official Publication of the American Association of Physical Anthropologists, 111(1), 45-68.

Williams, B. A., and Covert, H. H. (1994). New early Eocene anaptomorphine primate (Omomyidae) from the Washakie Basin, Wyoming, with comments on the phylogeny and paleobiology of anaptomorphines. American Journal of Physical Anthropology, 93(3), 323-340.

Williams, B. A., and Kirk, E. C. (2008). New Uintan primates from Texas and their implications for North American patterns of species richness during the Eocene. Journal of Human Evolution, 55(6), 927-941.

XIANG-XU, X., and DELSON, E. (1989). A new species of Dryopithecus from Gansu, China. Chinese Science Bullitin, 34, 223-229.

Yinyun, Z. (1982). Variability and evolutionary trends in tooth size of Gigantopithecus blacki. American Journal of Physical Anthropology, 59(1), 21-32.

Yuerong, P., Waddle, D. M., and Fleagle, J. G. (1989). Sexual dimorphism in Laccopithecus robustus, a late Miocene hominoid from China. American Journal of Physical Anthropology, 79(2), 137-158.

Zaim, Y., Ciochon, R. L., Polanski, J. M., Grine, F. E., Bettis III, E. A., Rizal, Y., ... and Marsh, H. E. (2011). New 1.5 million-year-old Homo erectus maxilla from Sangiran (Central Java, Indonesia). Journal of Human Evolution, 61(4), 363-376.

Zalmout, I. S., Sanders, W. J., MacLatchy, L. M., Gunnell, G. F., Al-Mufarreh, Y. A., Ali, M. A., ... and Gingerich, P. D. (2010). New Oligocene primate from Saudi Arabia and the divergence of apes and Old World monkeys. Nature, 466(7304), 360-364.

Zhang, Y., and Harrison, T. (2017). Gigantopithecus blacki: a giant ape from the Pleistocene of Asia revisited. American journal of physical anthropology, 162, 153-177.

Zhang, Y., Jin, C., Cai, Y., Kono, R., Wang, W., Wang, Y., ... and Yan, Y. (2013). New 400e320 ka Gigantopithecus blacki remains from hejiang cave, chongzuo City, guangxi, South China. Quaternary International, 30(1), e11.

Zhao, L. X., and Zhang, L. Z. (2013). New fossil evidence and diet analysis of Gigantopithecus blacki and its distribution and extinction in South China. Quaternary International, 286, 69-74.

Zijlstra, J. S., Flynn, L. J., and Wessels, W. (2013). The westernmost tarsier: A new genus and species from the Miocene of Pakistan. Journal of human evolution, 65(5), 544-550.

Zoological Laboratory (Cambridge, Mass.). Bulletin of the Museum of Comparative Zoology at Harvard College.

DRAFT

H. Supplementary references

78. CC Roseman, LK Delezene, The inhibitory cascade model is not a good predictor of molar size covariation. *Evol. Biol.* **46**, 229–238 (2019).
79. V Mitov, K Bartoszek, G Asimomitis, T Stadler, Fast likelihood calculation for multivariate gaussian phylogenetic models with shifts. *Theor. Popul. Biol.* **131**, 66–78 (2020).
80. MJ Hopkins, S Gerber, Morphological disparity. *Evol. developmental biology: A reference guide* pp. 965–976 (2021).
81. SP Blomberg, T Garland, AR Ives, Testing for phylogenetic signal in comparative data: behavioral traits are more labile. *Evolution* **57**, 717–745 (2003).
82. DC Adams, A generalized k statistic for estimating phylogenetic signal from shape and other high-dimensional multivariate data. *Syst. Biol.* **63**, 685–697 (2014).

DRAFT